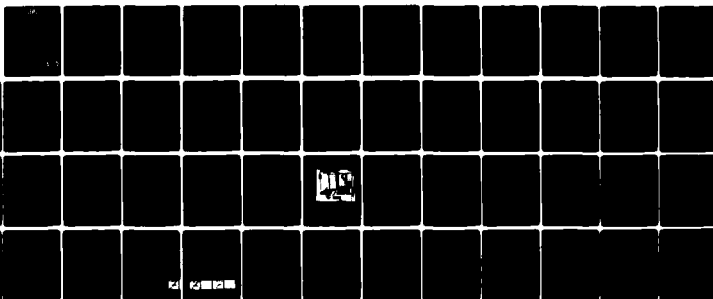


AD-A081 721

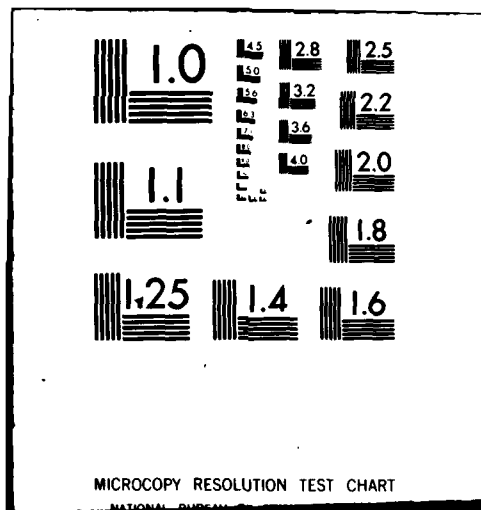
PHYSICS INTERNATIONAL CO SAN LEANDRO CA F/G 9/2  
FEASIBILITY STUDIES FOR A LOW-COST COMPUTERIZED DIAGNOSTIC SYST--ETC(U)  
DEC 78 D PELLINEN; S ASHBY DNA001-78-C-0333  
PIFR-1204 DNA-4796F NL

UNCLASSIFIED

1 1  
2 3 6 7 8



END  
DATE  
FILMED  
4-80  
DTIC



ADA 081 721

(12) **LEVEL** III  
R

AD-E 300 667

DNA 4796F

# FEASIBILITY STUDIES FOR A LOW-COST COMPUTERIZED DIAGNOSTIC SYSTEM FOR MODULAR PULSED ELECTRON ACCELERATORS

Physics International Company  
2700 Merced Street  
San Leandro, California 94577

31 December 1978

Final Report for Period 30 June 1978-31 December 1978

CONTRACT No. DNA 001-78-C-0333

APPROVED FOR PUBLIC RELEASE;  
DISTRIBUTION UNLIMITED.

THIS WORK SPONSORED BY THE DEFENSE NUCLEAR AGENCY  
UNDER FDT&E RMSS CODE B323078462 G37LAXYX96012 H2590D.

DDC FILE COPY.

Prepared for  
Director  
DEFENSE NUCLEAR AGENCY  
Washington, D. C. 20305

DTIC  
ELECTE  
MAR 12 1980  
S B D

80- 7 1 010

Destroy this report when it is no longer needed. Do not return to sender.

PLEASE NOTIFY THE DEFENSE NUCLEAR AGENCY,  
ATTN: STTI, WASHINGTON, D.C. 20305, IF  
YOUR ADDRESS IS INCORRECT, IF YOU WISH TO  
BE DELETED FROM THE DISTRIBUTION LIST, OR  
IF THE ADDRESSEE IS NO LONGER EMPLOYED BY  
YOUR ORGANIZATION.



631111

(18) LA 11, 5822

UNCLASSIFIED

SECURITY CLASSIFICATION OF THIS PAGE (When Data Entered)

17 REPORT DOCUMENTATION PAGE		READ INSTRUCTIONS BEFORE COMPLETING FORM
1. REPORT NUMBER DNA 4796F, HD-E300 6671	2. GOVT ACCESSION NO.	3. RECIPIENT'S CATALOG NUMBER
4. TITLE (and Subtitle) FEASIBILITY STUDIES FOR A LOW-COST COMPUTERIZED DIAGNOSTIC SYSTEM FOR MODULAR PULSED ELECTRON ACCELERATORS.	5. TYPE OF REPORT & PERIOD COVERED Final Report for Period 30 June 78 - 31 Dec 78	6. PERFORMING ORG. REPORT NUMBER PIFR-1204
7. AUTHOR(s) D. Pellinen S. Ashby	8. CONTRACT OR GRANT NUMBER(s) DNA 001-78-C-0333 <sup>new</sup>	
9. PERFORMING ORGANIZATION NAME AND ADDRESS Physics International Company 2700 Merced Street San Leandro, California 94577	10. PROGRAM ELEMENT, PROJECT, TASK AREA & WORK UNIT NUMBERS Subtask G37LAXYX960-12	
11. CONTROLLING OFFICE NAME AND ADDRESS Director Defense Nuclear Agency Washington, D.C. 20305	12. REPORT DATE 31 December 1978	
14. MONITORING AGENCY NAME & ADDRESS (if different from Controlling Office)  (12) 561	13. NUMBER OF PAGES 56	15. SECURITY CLASS (of this report) UNCLASSIFIED (17) 4796F
16. DISTRIBUTION STATEMENT (of this Report)  Approved for public release; distribution unlimited.		
17. DISTRIBUTION STATEMENT (of the abstract entered in Block 20, if different from Report)		
18. SUPPLEMENTARY NOTES  This work sponsored by the Defense Nuclear Agency under RDT&E RMSS Code B323078462 G37LAXYX96012 H2590D.		
19. KEY WORDS (Continue on reverse side if necessary and identify by block number)  Diagnostics                      Voltage Monitors Electron Accelerators          Current Monitors Computerized Diagnostics		
20. ABSTRACT (Continue on reverse side if necessary and identify by block number)  We have developed a low-cost, nanosecond response diagnostic system for measuring the performance of a pulsed electron accelerator module. The system uses inexpensive sensors hardwired to electronic circuits, which are interfaced to a digital computer. Projections and cost estimates were made for a 300-module system incorporating this diagnostic system.		

DD FORM 1 JAN 73 1473 A EDITION OF 1 NOV 65 IS OBSOLETE

UNCLASSIFIED

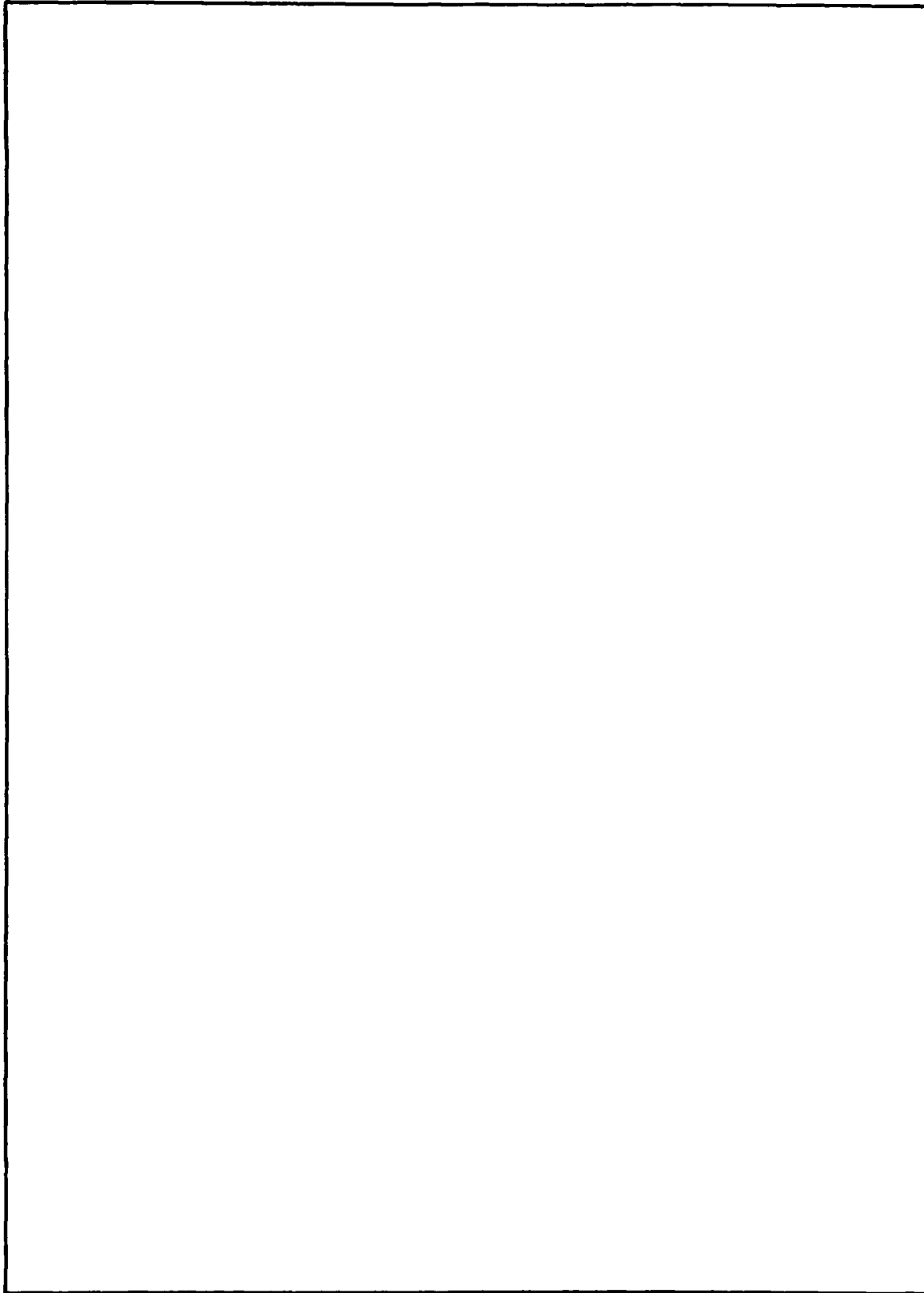
SECURITY CLASSIFICATION OF THIS PAGE (When Data Entered)

202111

13

UNCLASSIFIED

SECURITY CLASSIFICATION OF THIS PAGE(When Data Entered)



UNCLASSIFIED

SECURITY CLASSIFICATION OF THIS PAGE(When Data Entered)

## PREFACE

The work described in this report was performed under Contract DNA001-78-C-0333 awarded by the Defense Nuclear Agency. This program was managed by D. G. Pellinen and supervised by P. W. Spence. The majority of the experimental work was conducted by S. A. Ashby. We acknowledge the assistance of K. Nielsen, P. D'A. Champney, P. Gillis, J. Kishi, and W. Wagonlander, who conducted the experiments on the module. Assistance in preparing this report was given by G. Lawler and C. Childers.

The need for a program to economically diagnose an MBS system was recognized by the MBS Project Officer LCDR. Otis Cole who initiated the project and monitored it through the experimental program. Mr. George Baker succeeded LCDR. Cole as Project Officer in the later stages of the program.

ACCESSION for	
NTIS	White Section <input checked="" type="checkbox"/>
DDC	Buff Section <input type="checkbox"/>
UNANNOUNCED	<input type="checkbox"/>
JUSTIFICATION _____	
BY _____	
DISTRIBUTION/AVAILABILITY CODES	
Dist. A/R/L and/or SPECIAL	
A	

## CONTENTS

	<u>Page</u>
SECTION 1 INTRODUCTION	5
SECTION 2 BASIC IDEAS FOR A DIAGNOSTIC SYSTEM AS APPLIED TO AN 8-PULSELINE MBS MODULE	7
2.1 Logic of Diagnostics System for MBS	7
2.2 Detectors and Circuitry	21
2.3 Data Interfaces	28
2.4 General Comments on Data Acquisition Circuitry	31
SECTION 3 EXPERIMENTAL PROGRAM	36
3.1 Program Plan and Objectives	36
3.2 Components	38
3.3 Diagnostic Master Trigger	39
3.4 Faraday Enclosures (Screen Rooms)	39
3.5 3-D Results	40
SECTION 4 COST PROJECTIONS FOR THE SXTF	45
BIBLIOGRAPHY	51



## ILLUSTRATIONS

<u>Figure</u>		<u>Page</u>
1	MBS Pulser Block Diagram	9
2	Logic Diagram for Debugging Pulser	10
3	Single MBS Pulseline with Diagnostics in Place	12
4	Diagnostic Placement--8-Module MBS System	13
5	Wiring Diagram--Data Acquisition System for 8-Module MBS System	14
6	Marx Generator Diagnostic Circuitry	15
7	Charging Diagram for Marx in Normal and Fault Conditions	17
8	Normal Trigger Waveform and Normal Waveform with Three Malfunction Conditions	22
9	Pulse Charge Waveform with Waveform from Track-and-Hold Circuit	24
10	Block Diagram Track-and-Hold Circuit for Measuring Pulse Charge	25
11a	Diode Voltage, $V_I$	27
11b	Diode Current Waveform, $I_D$	27
11c	Cathode Current, $I_C$	27
12	Prototype CAMAC Data Acquisition System	30
13	Methods of Interfacing CAMAC to the Computer	32
14	Data Acquisition System for Single MBS Module Using Commercial Circuits	34
15	Diagnostic Development for Advanced Simulators	37
16	Summary of Data from MBS Pulses 706 to 712	41

## TABLES

<u>Table</u>		<u>Page</u>
1	Table of Postulated Values for Integrating Voltage and Time-To-Digital Converters Under Various Fault Modes	19
2	Normalized Data from Shots 706 to 712	43
3	Differences in Time Between Fixed Points on MBS	44
4	Module Diagnostics for 300-Module MBS	47
5	Marx Diagnostics (38 Marxes) for 300-Module MBS	48
6	CAMAC Crates and Interface Hardware	49
7	Projected Total Component Costs for MBS Pulser Instrumentation	49

## SECTION 1

### INTRODUCTION

We have developed a new computerized diagnostic system for the pulser modules on MBS. This diagnostic system uses electronic circuits to measure machine performance at critical points. The voltage outputs of these circuits are converted to digital form and directly read by a computer. The major advantages of this system are:

1. A single data channel can be completely implemented for about \$300 compared with  $\approx$  \$5 K for an oscilloscope or  $\approx$  \$20 K for a transient analyzer.
2. The system is more accurate than an oscilloscope or transient analyzer.
3. Operation is fully computerized and will require a minimum number of personnel to operate.
4. The system is scalable to very large multi-module generators.

The approach used was to locate areas where problems could occur in the MBS modules and place appropriate nanosecond response transducers, such as voltage and current sensors, at these locations. These sensors are connected to circuits that will record and hold the parameter we are measuring, such as time, a peak amplitude, or an integral of a voltage. The data are converted to digital form, read, and processed by a digital computer.

We assembled a prototype system of this type using commercial equipment and tested it on the MBS module under development. Additional diagnostic system data were collected for approximately two

months while the diagnostic system ran automatically under computer control. We found that by using good grounding and shielding techniques, we could use conventional inexpensive hardwired connections to transmit fast signals without causing spurious responses or damage to the circuitry or computer.

We also developed a comprehensive plan for a diagnostic system for a 300-module MBS. This system has nanosecond response transducers located at critical points in the modules, Marx pulse charge generators, and triggering system; the entire system is comprised of 2176 fast transducers and 156 essentially dc detectors being read out by 3452 fast circuits and 156 slow circuits. The total estimated component cost for this diagnostic system is about \$780 K.

Section 2 of this report discusses the evolution of this diagnostic system approach in the context of the FY79 8-pulseline MBS module. Section 3 describes the experimental work performed during this contract and presents data establishing the feasibility of such a system. A discussion of the full extension of this approach to a 300-pulseline MBS generator, including component cost estimates, is given in Section 4.

## SECTION 2

### BASIC IDEAS FOR A DIAGNOSTIC SYSTEM AS APPLIED TO AN 8-PULSELINE MBS MODULE

In this section, we first review the rationale and cost benefits of a selected digital data acquisition approach for MBS instrumentation. This approach is illustrated by reviewing the proposed diagnostic system for an 8-pulseline module of MBS to be built in FY79. Sensor requirements, sensor locations, a catalog of fault modes which could be identified with the diagnostic system, a description of sensor types and electronic circuits, and recommended computer interface hardware are discussed.

#### 2.1 LOGIC OF DIAGNOSTICS SYSTEM FOR MBS

2.1.1 Discussion of Full Analog Versus Selected Digital Recording Approach. When the MBS was first described as having 300 modules, an immediate question arose--how could one determine whether the modules were functioning correctly? With existing technology, the minimum diagnostics to determine a module malfunction would consist of a radiation detector and oscilloscope for each module. This approach would cost 1.5 million dollars (300 x \$5,000 per scope channel), plus 6 to 8 people to operate the equipment and reduce the data. Such a diagnostics system would tell us only that the module malfunctioned, but nothing about why, whether the malfunction was minor, whether it was a random event, or whether it could damage the source. Certain malfunction modes have the potential to physically damage the source on a succeeding shot, so it would be important that the fault be identified immediately.

Clearly a more complete set of diagnostics is required to define the nature of malfunctions and pinpoint repairs or corrective action. To do this adequately using historical technology, i.e., oscilloscopes or transient analyzers, would cost more than the facility itself and leave the operators with an unmanageable mountain of data. The approach we took in this program was prompted by review of normal troubleshooting methods for a malfunctioning machine using oscilloscope traces.

First of all, we conceived the accelerator as depicted in the block diagram shown in Figure 1. Normally monitors are situated to measure the inputs to a block and the outputs from the block that form the inputs to the next block. Troubleshooting consists of asking the following questions:

- Did the correct inputs enter block N?  
    If yes
- Did the correct output exit?  
    If yes
- Go to Module (N+1)  
    If no
- Malfunction location identified. Determine cause of malfunction.

This model is very similar to a logic diagram for a computer (Figure 2) and suggests very strongly that this type of approach would be relatively easy to computerize.

Second, in the process of debugging a machine, one makes use of a fair number of oscilloscope traces (full analog data recovery), but usually only one or two pieces of information on each trace (selected digital points) are used to quantify generator operation. Since a fully equipped, fast oscilloscope costs about \$5,000 per channel, this is a very expensive way of measuring a single data point to a maximum accuracy of 3 percent. In the proposal (PIP-1982, April 1978), we initially estimated the cost of building electronic

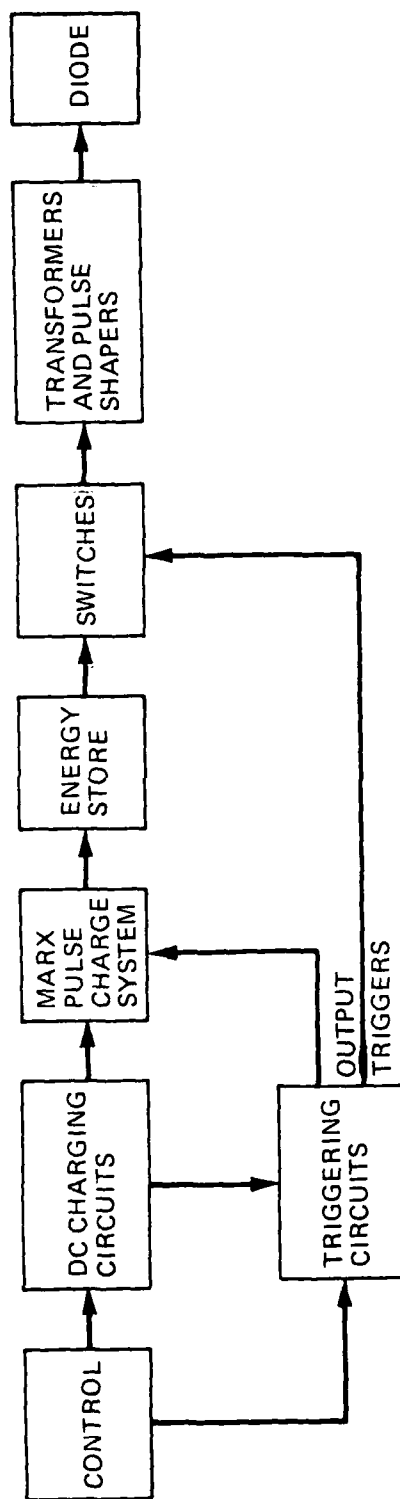


Figure 1 MBS Pulser block diagram.

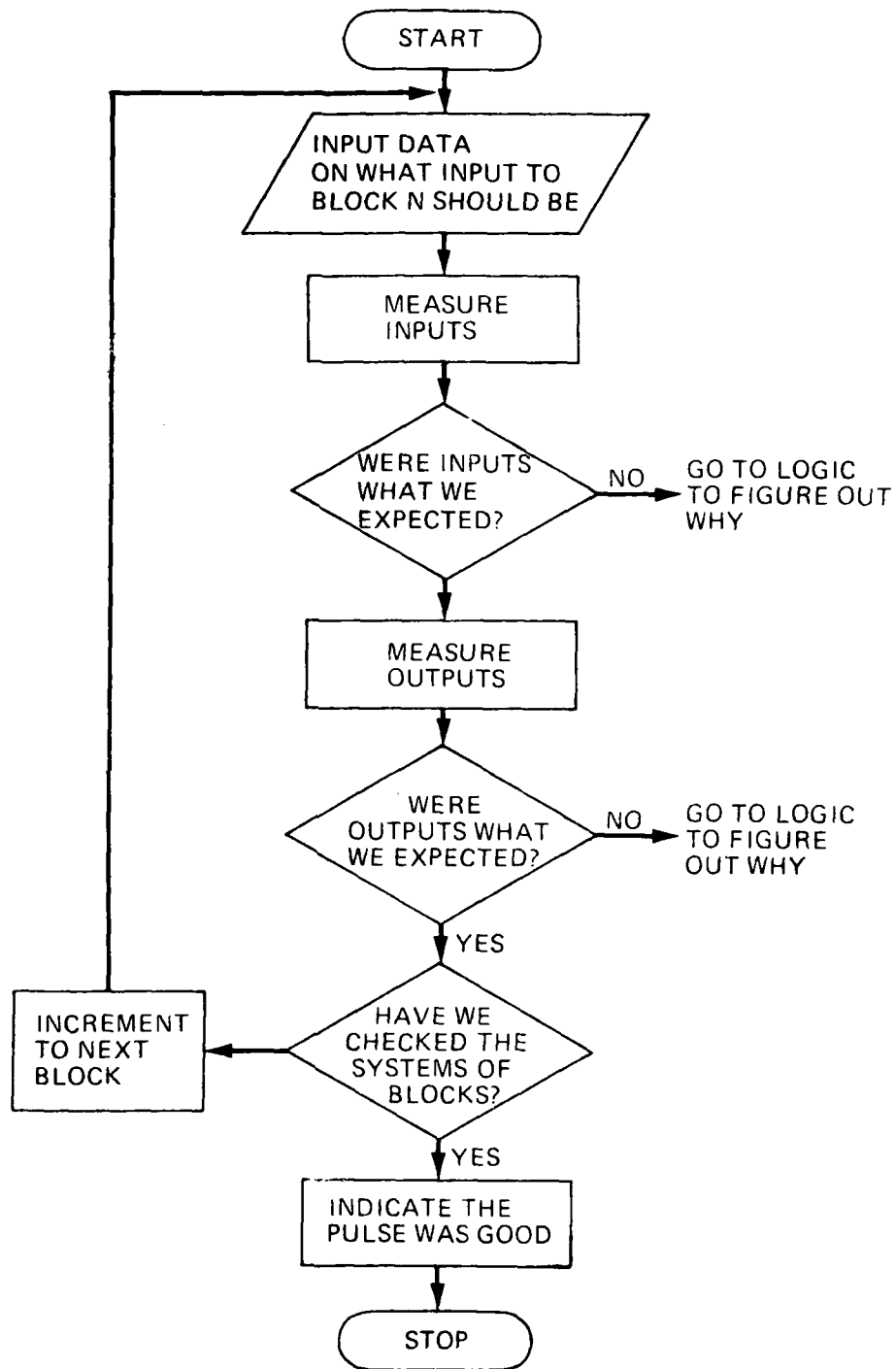


Figure 2 Logic diagram for debugging pulser.



circuitry to measure a single digital point with improved accuracy (< 1 percent) at \$100 to \$200 per channel. We determined that many of these circuits are also commercially available as CAMAC modules (originally developed to measure radiation outputs from particle accelerators) at a cost of about \$150 per channel.

#### 2.1.2 Diagnostic System Logic as Applied to 8-Pulseline MBS.

We illustrate below how this diagnostic system approach can be used on the 8-pulseline MBS unit to be built in FY79. Figure 3 shows a single MBS pulseline with the proposed diagnostic package in place. Figure 4 shows a block diagram of 8 modules with diagnostics installed. Figure 5 shows a block diagram of the module diagnostics monitoring package. Figure 6 shows a block diagram of the diagnostics package for the Marx Generator and triggering circuit.

We will now discuss the individual monitor requirements and rationale for instrumentation of each functional block in the MBS system shown in Figure 4.

Master Timing Generator. Any synchronized machine requires triggers to initiate switch closures, starting the power flow in the machine. Sensors will be placed on the trigger output cables going to the Marx and modules. The sensors will be monitored for the time difference between initiation and outputs, and for integrals. These are very important measurements, since these trigger pulses are responsible for machine synchronization and, to a great degree, whether the module will function at all.

$V_{MT}$ , the trigger to the Marx, would be timed to ensure that it arrives on time and the integral of the voltage measured to determine that the trigger cable and system are not shorted, disconnected, or broken.

DC Charging Circuits--Voltage and Current on the Plus and Minus Legs of the Marx. These are important measurements since the energy stored in the Marx is  $1/2 qV^2$ . If the stored charge,  $i\Delta t$ , is plotted versus voltage on a terminal or digitized within the computer, it

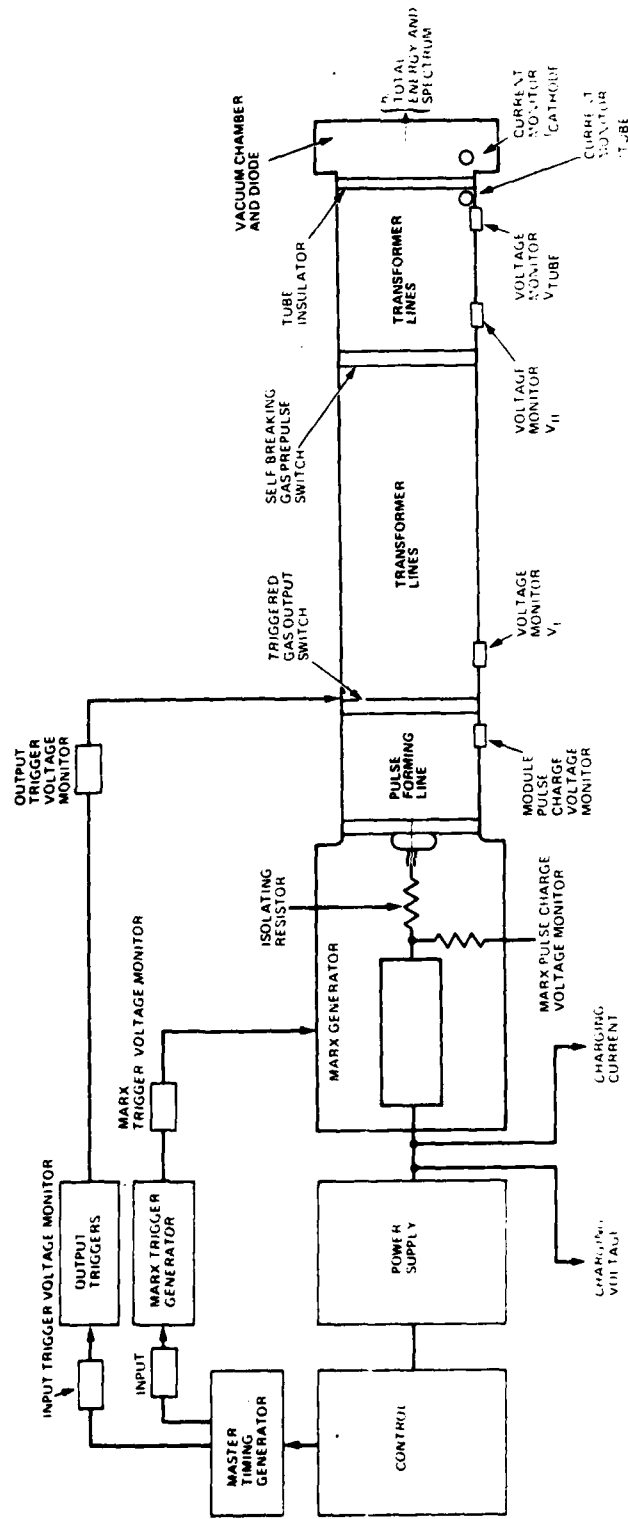


Figure 3 Single MBS pulseline with diagnostics in place.

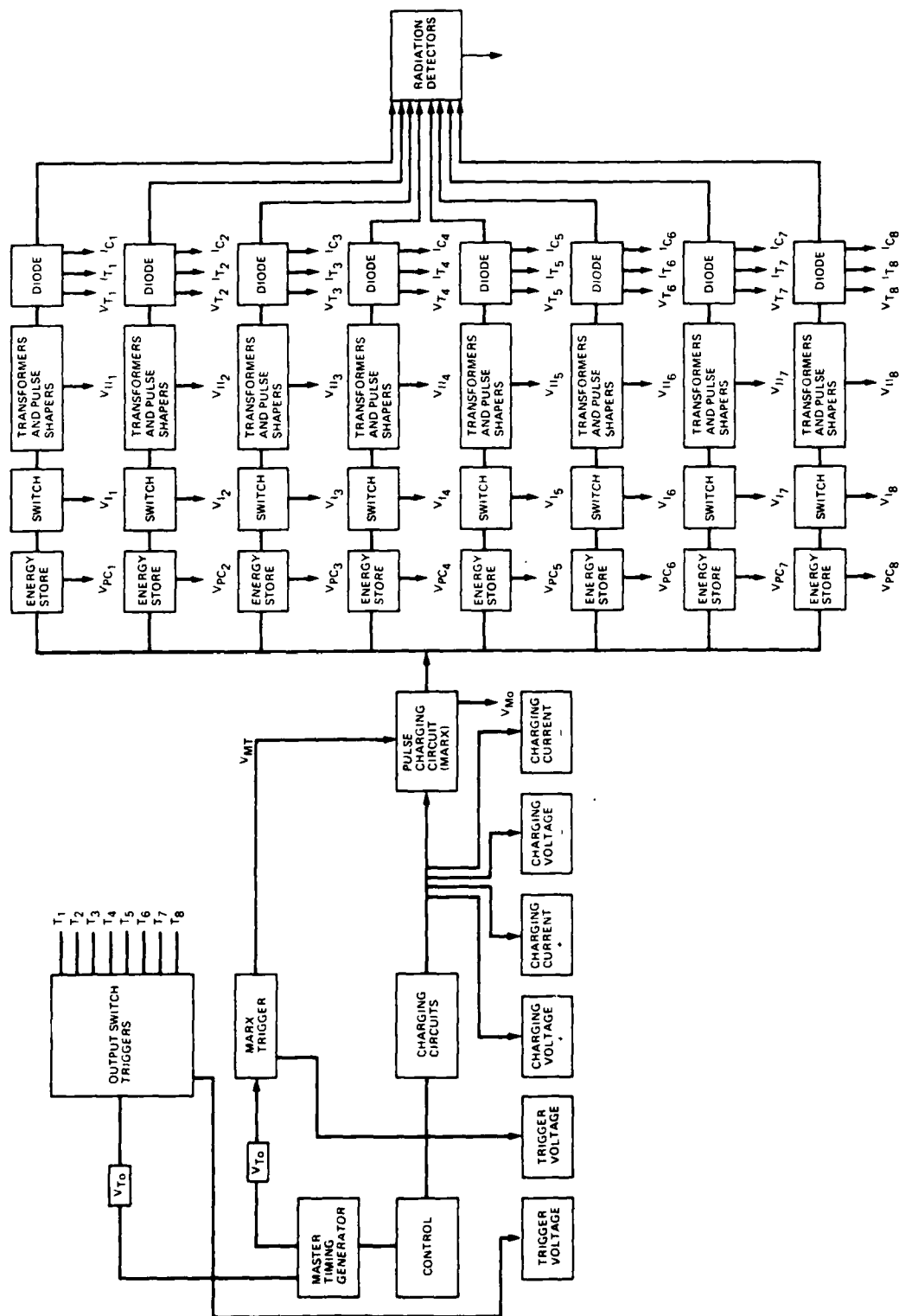


Figure 4 Diagnostic placement--8-module MBS system.

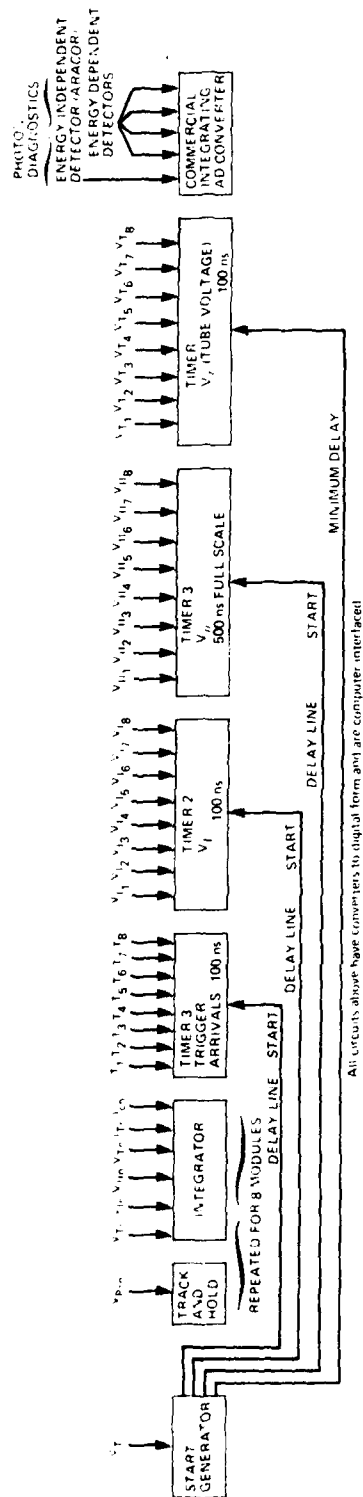


Figure 5 Wiring diagram--data acquisition system for 8-module MBS system.

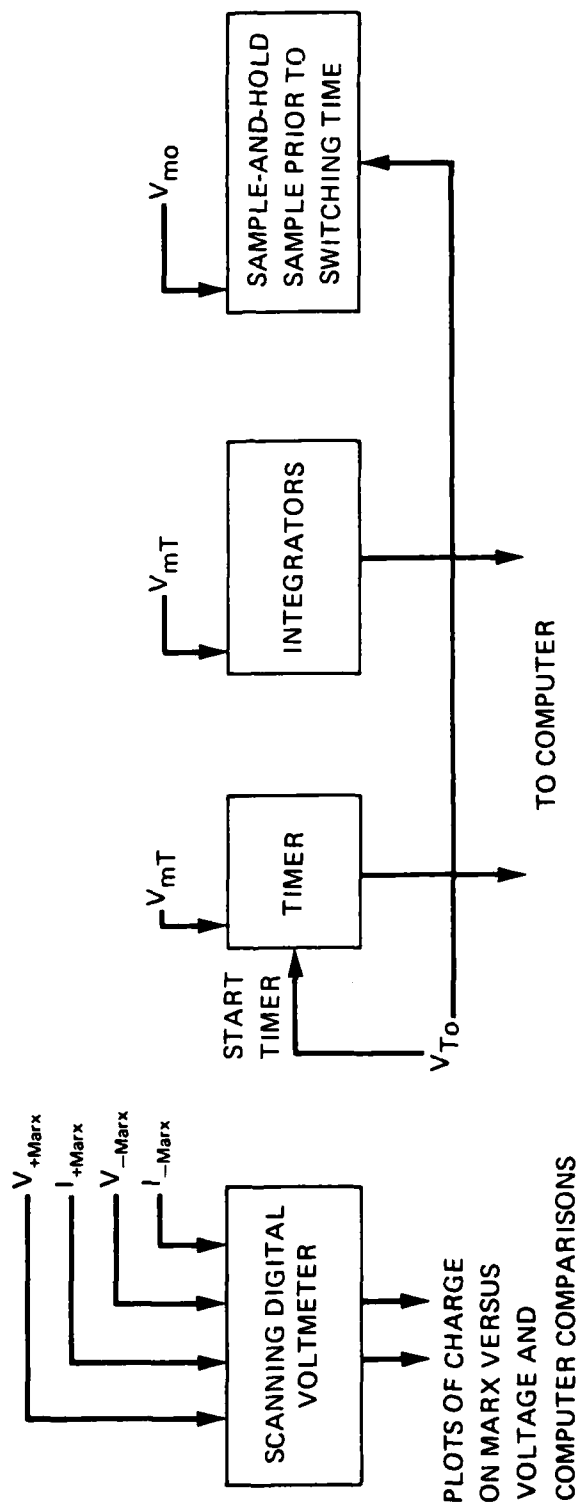


Figure 6 Marx generator diagnostic circuitry.

is an indicator of the condition of the Marx. The plot should be nominally linear. If the plot shows an abnormally low charge for a given voltage, it implies that capacitors are disconnected or charging resistors have broken contact. An abnormally high slope on the charge-voltage curve beginning at a certain voltage implies that a spark gap is breaking down. Deviations from linearity indicate a bad contact.

A high slope throughout the charge indicates a leaky or shorted capacitor or poor quality oil. Examples of these cases are plotted in Figure 7. Certain of these malfunctions would require the computer to immediately alert the operator to take the Marx out of service for repairs; the computer might possibly adjust gas pressure in the Marx automatically.  $V_{mo}$  is the Marx output voltage measured before any isolating resistors to the individual modules. An abnormally low voltage at  $V_{mo}$  combined with abnormally low pulse charge voltages on the  $V_{pcn}$  monitors would imply a switching malfunction in the Marx. A high reading on  $V_{mo}$  combined with an abnormal reading of  $V_{pcn}$  on single modules would imply that one line was badly connected. A high reading on  $V_{mo}$  combined with fairly uniform lower readings on the module pulse charge voltages  $V_{pcn}$  would imply that the isolating resistors were of too high a value.

Energy Store. The input to the energy store is  $V_{mo}$ . The module output is the pulse charge voltage  $V_{pcn}$  and  $V_{In}$ .  $V_{pcn}$  is the voltage measured several nanoseconds before the voltage drops when the switch closes. Possible fault modes indicated by  $V_{pcn}$  are: (1) low stored energy, indicated by a low reading on  $V_{pcn}$  compared with the dc charging voltage and the  $V_{mo}$ ; this problem could be caused by a charging resistor with too high a value or conductive water; (2) an electrical breakdown through the water or along the switch envelope, indicated by a slightly low reading on  $V_{pcn}$  and a low or negligible output on  $V_{In}$  accompanied by

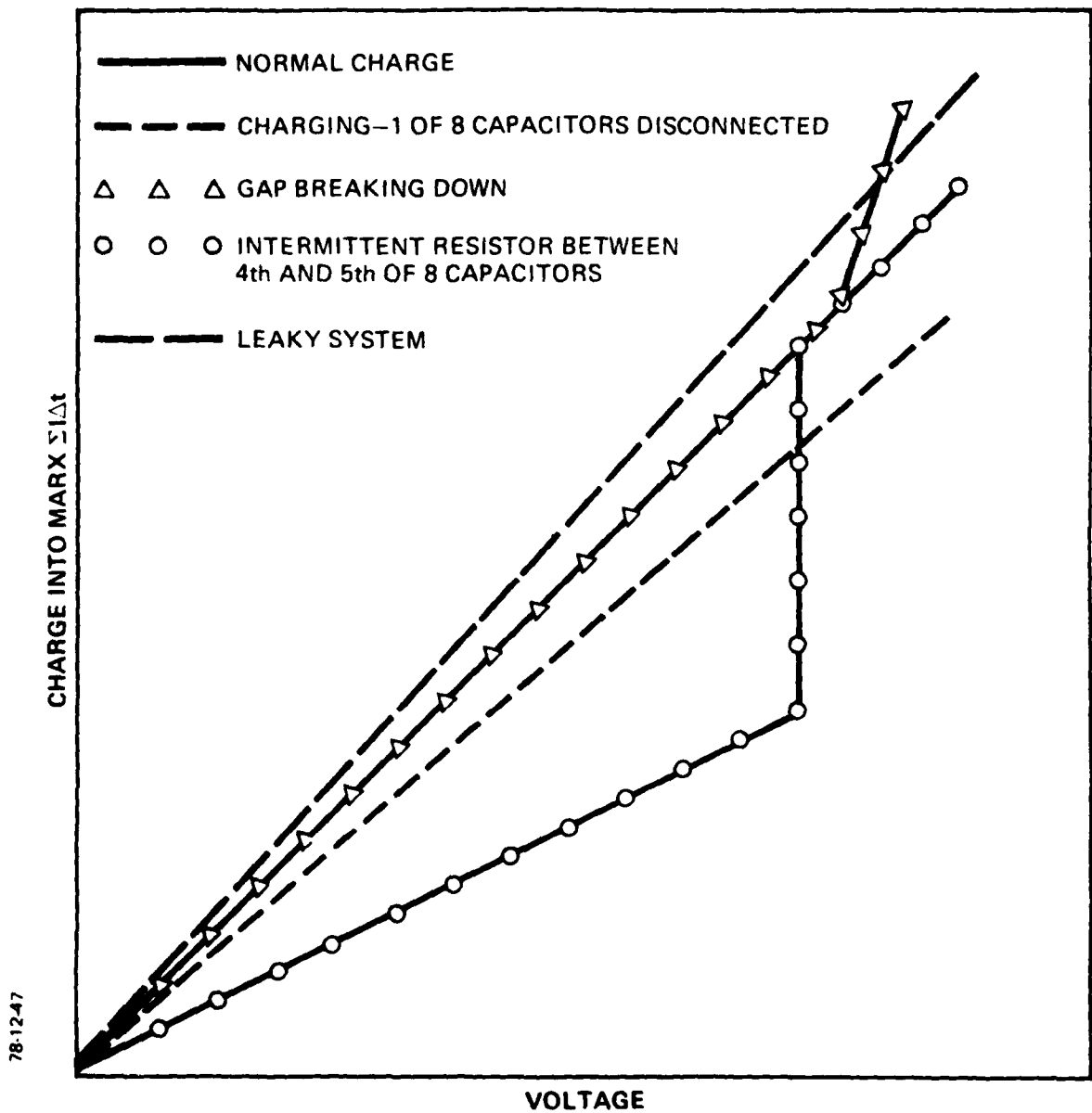


Figure 7 Charging diagram for Marx in normal and fault conditions.

closure before the trigger and later monitors (see Table 1, line 8). Both the voltage at the breakback and the time when the breakback occurs should be measured. The computer should keep a record of line breakdowns, and if they occur excessively, on consecutive pulses, or at very low voltages, the module should be removed from service.

The Switch. The input to the switch functional block is stored energy measured by  $V_{pcn}$ , and the trigger, the arrival time and quality of which are measured by  $V_{Tn}$ . The output measured is  $V_{In}$ , the switch output voltage. The integral of amplitude of  $V_{In}$  would be determined. The time when the switching occurred would be measured by the breakback on  $V_{pcn}$ . Malfunction modes that would be indicated are the water breakdown described in the energy store section, and the switch self-closing. A self-break on the switch would be indicated by a closure time before the trigger and essentially normal amplitudes down the pulse line (see Table 1, line 7). A triggered switch closure at a slightly abnormal time would be indicated by normal integrals and abnormal times propagated down the pulse line. The abnormal switching would affect the simultaneity of the modules and degrade the radiation output risetime (see Table 1, lines 12 and 13).

Transformer and Pulse Shaper Functional Block. The input information to this block is measured by outputs from  $V_{In}$ . The outputs from this stage are measured at  $V_{IIn}$  and also at  $V_{Tn}$  and  $I_{Tn}$ . Potential problem areas through this stage are: (1) losses due to conductive water; (2) breakdown in the water or on the water plastic interface; and (3) incorrect closure of the prepulse switch. The loss condition would show as low voltage levels throughout the system and probably excessive delay in prepulse switch closure as measured by  $V_T$  and time of pulse arrival (Table 1, line 24). A



TABLE 1

TABLE OF POSTULATED VALUES FOR INTEGRATING VOLTAGE AND TIME-TO-DIGITAL CONVERTERS UNDER VARIOUS FAULT MODES\*

Malfunction	V Pulse Charge on Module		V Trigger		V <sub>I</sub>		V <sub>II</sub>		Diode Voltage		Diode Current		Cathode Current	
	$\mu\text{Vdt}$	$\mu\text{V}$	$\mu\text{Vdt}$	$\mu\text{V}$	$\mu\text{Vdt}$	$\mu\text{V}$	$\mu\text{Vdt}$	$\mu\text{V}$	$\mu\text{Vdt}$	$\mu\text{V}$	$\mu\text{Vdt}$	$\mu\text{V}$	$\mu\text{Vdt}$	$\mu\text{V}$
1. Normal shot	500	50.00	500	50.00	500	500	250.0	500	50.00	500	500	500	500	500
2. 10 percent low pulse charge	450	45.00	550	55.00	450	440	251.2	440	51.20	440	440	440	440	440
3. Isolating resistor low	497	49.70	480	48.00	524	524	249.4	525	49.40	525	525	525	525	525
4. Isolating resistor high	503	50.30	520	52.00	476	476	250.6	474	50.60	474	474	474	474	474
5. 10 percent high pulse charge	550	55.00	450	45.00	550	550	248.8	560	48.80	560	560	560	560	560
6. 10 percent high pulse charge, triggered switching	500	50.00	500	50.00	500	500	250.0	500	50.00	500	500	500	500	500
7. Normal pulse charge, 20 ns self-fire, all modules	500	50.00	500	50.00	500	500	250.0	500	50.00	500	500	500	500	500
8. Normal pulse charge, 20 ns breakdown, 20 ns	500	50.00	500	50.00	500	500	250.0	500	50.00	500	500	500	500	500
9. Normal pulse charge, 20 ns breakdown, 20 ns	500	50.00	500	50.00	500	500	250.0	500	50.00	500	500	500	500	500
10. No trigger from generator	500	50.00	500	50.00	500	500	250.0	500	50.00	500	500	500	500	500
11. Trigger cable shorted	500	50.00	500	50.00	500	500	250.0	500	50.00	500	500	500	500	500
12. Trigger cable open at TIG	500	50.00	500	50.00	500	500	250.0	500	50.00	500	500	500	500	500
13. High main switch pressure	500	50.00	500	50.00	500	500	250.0	500	50.00	500	500	500	500	500
14. Low main switch pressure	500	50.00	500	50.00	500	500	250.0	500	50.00	500	500	500	500	500
15. High prepulse switch pressure	500	50.00	500	50.00	500	500	250.0	500	50.00	500	500	500	500	500
16. Low prepulse switch pressure	500	50.00	500	50.00	500	500	250.0	500	50.00	500	500	500	500	500
17. Water breakdown, 30 ns into pulse	500	50.00	500	50.00	500	500	250.0	500	50.00	500	500	500	500	500
18. Prepulse switch set too high, switch break to ground	500	50.00	500	50.00	500	500	250.0	500	50.00	500	500	500	500	500
19. Prepulse switch break on pulse charge diode short into pulse	500	50.00	500	50.00	500	500	250.0	500	50.00	500	500	500	500	500
20. Insulator flash > 20 ns into pulse	500	50.00	500	50.00	500	500	250.0	500	50.00	500	500	500	500	500
21. Diode short at time 0	500	50.00	500	50.00	500	500	250.0	500	50.00	500	500	500	500	500
22. Diode impedance > 20% high	500	50.00	500	50.00	500	500	250.0	500	50.00	500	500	500	500	500
23. Diode impedance > 20% low	500	50.00	500	50.00	500	500	250.0	500	50.00	500	500	500	500	500
24. Prefire 100 ns early	490	49.00	510	51.00	490	490	251.0	490	51.00	490	490	490	490	490
25. Lossy water, normal switch	500	50.00	500	50.00	500	500	250.0	500	50.00	500	500	500	500	500

\*The majority of these conditions were not actually observed in testing but inferred from experience with other accelerators. The table is intended to illustrate the distinct pattern of outputs one would expect from these sensors and converters. These values should actually be measured as part of the software development program by deliberately setting up a series of malfunctions.

breakdown in the lines would show itself as normal pulse charge and voltage  $V_{In}$  followed by low readings on  $V_{IIn}$ ,  $V_{Tn}$ , and  $I_{Tn}$ , (Table 1, lines 16 and 17). This problem is normally caused by a gas bubble in the line, misassembly, or a cracked switch leaking gas. The computer should definitely be programmed to look for these modes. Incorrect closure time is indicated as a change in the time interval between  $V_{In}$  and  $V_{Tn}$  accompanied by a change in  $V_{IIn}$ ,  $V_{Tn}$ , and  $I_{Tn}$  (see Table 1, lines 14 and 15).

Diode. The wave traveling up the line to the diode has its shape defined by system geometry and to a slight degree by the delays and characteristics of the switches. At the diode, various load conditions result in significant waveform changes. Accordingly, we have situated three instruments near each diode--  $V_{Tn}$ , the diode voltage monitor;  $I_{Tn}$ , the current monitor located before the insulator; and  $I_{cn}$ , the cathode current monitor.  $V_{Tn}$  is instrumented with an integrating analog-to-digital converter and a time-to-digital converter to measure voltage arrival time and prepulse switch timing.

$I_{Tn}$  and  $I_{cn}$  are instrumented with integrating analog-to-digital converters. Among the possible problems at the diode are: (1) changes in output photon energy caused by small changes in diode spacing and size; (2) dirty insulators, which result in surface flashover robbing the diode of energy; (3) misadjustment or damage in the cathode, which can result in a diode short and therefore zero energy transfer to the diode. The main conditions we can determine from diode diagnostics are normal pulses (Table 1, line 1) insulator flashes, (Table 1, line 19), diode shorts (Table 1, line 20) and total diode energy and mean energy. We will discuss response to various conditions when we discuss detectors.

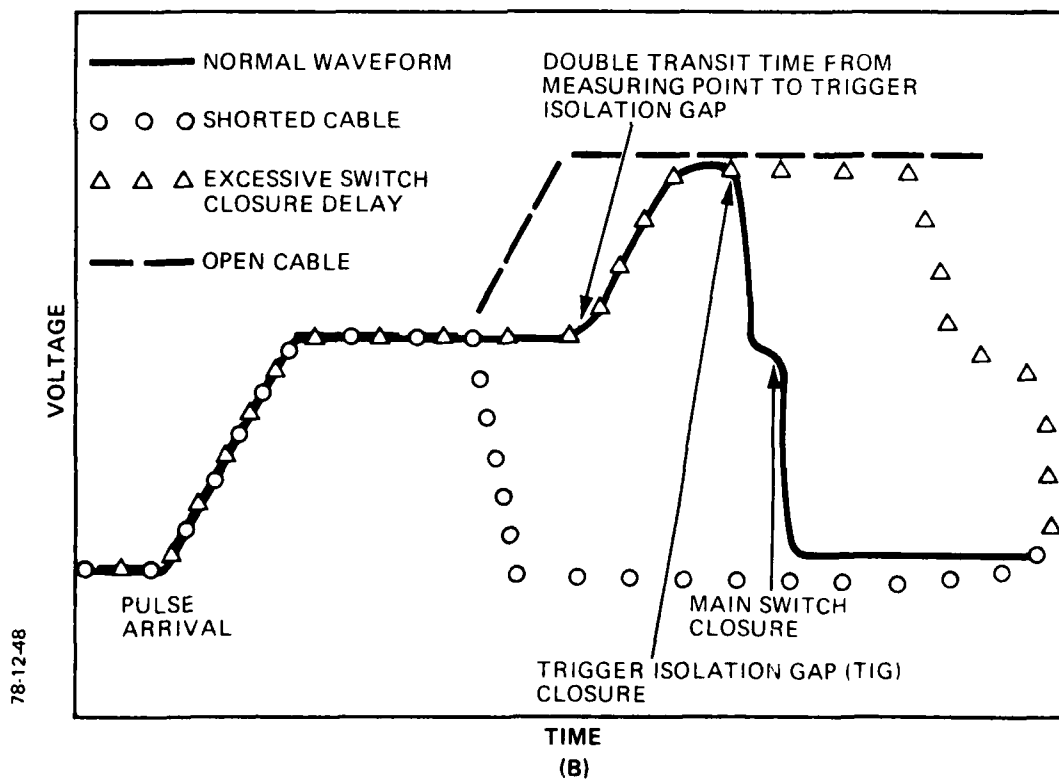
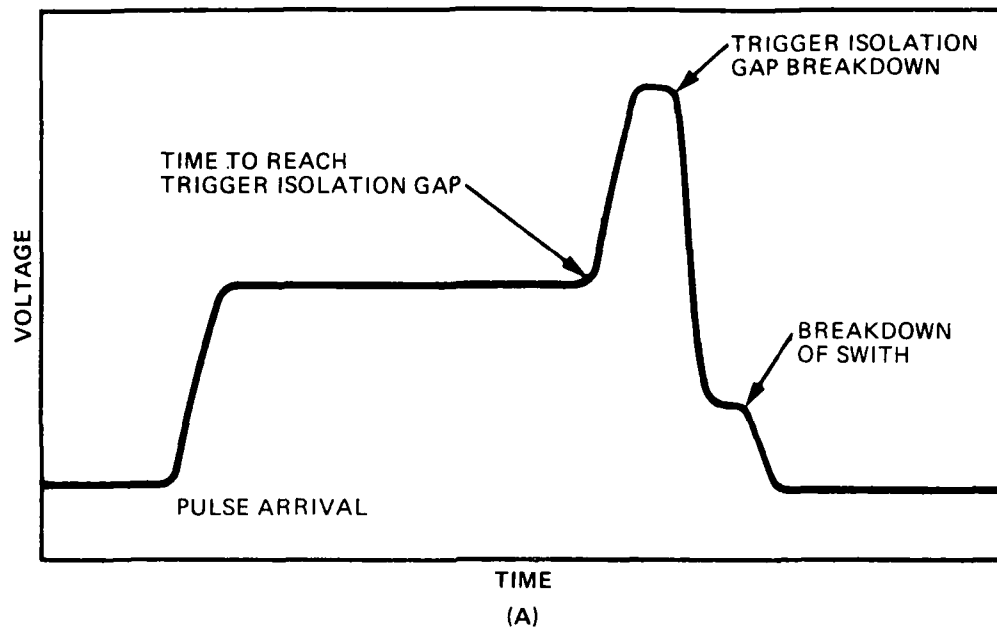
Radiation Detection. A number of devices could be used; the most likely candidates would be similar to the flat response pin diode for total energy, and Ross filtered pin diodes or photo-multipliers for developing a "handle" on the spectrum. Measuring the output of this type of device to obtain total energy is trivial since commercial charge integrating analog-to-digital converters designed to do this are available for about \$150 per channel with 12 channels per module. This type of device offers the advantage of data that are available within a second or two and included on printouts with the pulser performance data. This type of radiation detection system on the SXTF module would be convenient because it would give both operator and user an immediate reading on the radiation fluence and spectrum.

## 2.2 DETECTORS AND CIRCUITRY

We will describe the individual devices actually used as sensors, along with the circuitry for each device we intend to use.

Trigger Output Monitor. Typical trigger output waveforms will appear similar to that shown in Figure 8. They will be measured by a capacitive voltage divider connected over the coax cable feeding the trigger into the module. This output will be measured with a time-to-digital converter measuring the pulse arrival time and a charge integrating analog-to-digital converter. Figure 8 shows how the integral will change with fault modes. (See also Table 1, lines 9, 10, and 11.) Both Marx and module triggers will be monitored in this fashion.

Marx Output Voltage Monitor. The Marx generator output voltage provides a measure of the performance of the Marx and indicates the amount of energy available from the Marx. Since the individual pulse forming lines are resistively isolated from the



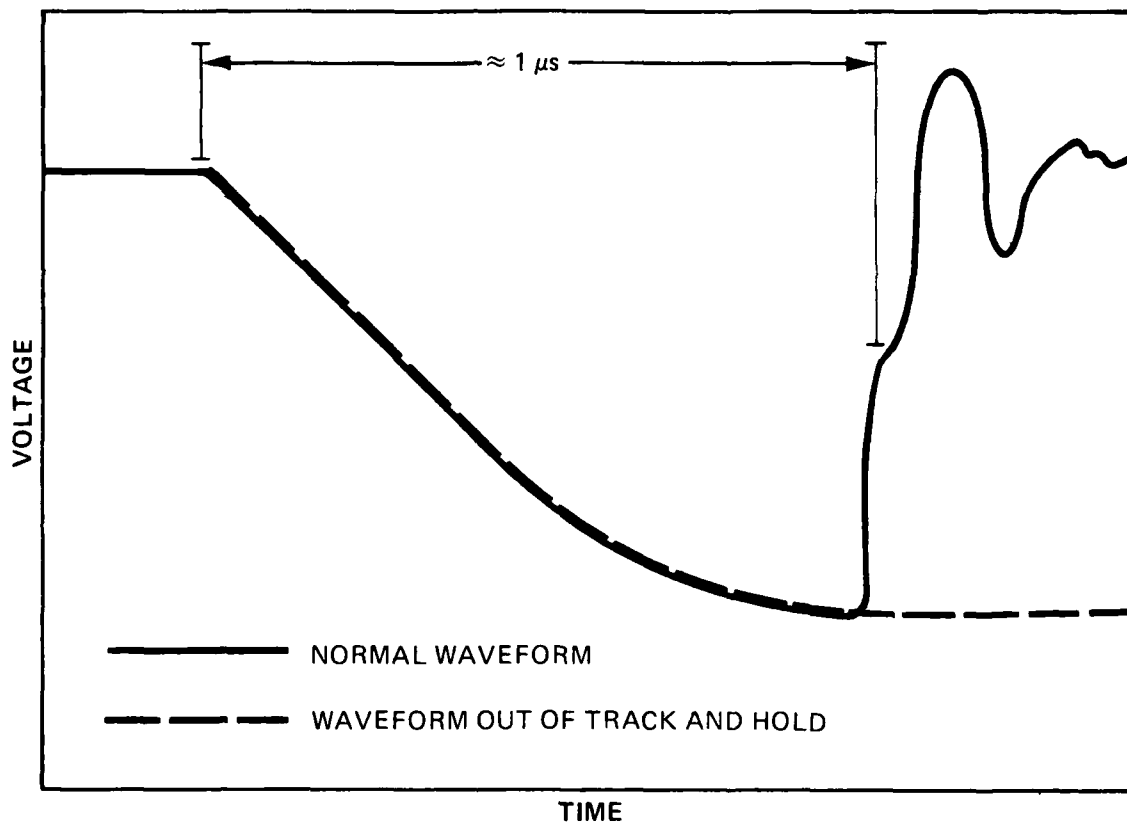
78-12-48

Figure 8 (a) Normal trigger waveform and (b) Normal waveform with three malfunction conditions.

Marx, the Marx output voltage is not necessarily a good measure of energy stored in the lines. Probably the best way to measure the Marx output voltage  $V_{mo}$  is with a sample-and-hold circuit gated somewhat before the trigger pulse to the lines arrives. Measuring Marx output with sample-and-hold triggered at a fixed time provides a measure of security against spuriously low measurements from the gate being triggered by a module prefiring. The transducer would probably be a copper sulfate resistor-divider network.

Module Pulse Charge Voltage Monitor ( $V_{pcn}$ ). This device measures the voltage on the pulse forming line. We are actually interested in knowing the voltage on the line at the instant of switching, since the stored energy of the line is  $1/2 CV^2$ . A typical waveform is shown in Figure 9. The waveform is approximated by  $V = V_0 (1 - \cos \omega t)$  until the main switch closure, when the voltage will drop to one-half its prior value in 10 to 15 ns. The best way to measure this waveform would be to develop a track-and-hold circuit that could be triggered to track on the positive slewing transient. The "held" voltage would be converted to digital form. This circuit does not require the high-frequency-response (and high-priced) input amplifiers that an adequate sample-and-hold circuit would require. The track-and-hold would give correct data on machine malfunction conditions as long as the positive breakback occurred.

Developing these circuits is the most logical and economical method for pulse charge diagnostics for the full MBS module. The block diagram for the pulse charge measuring circuit is shown in Figure 10. The circuit would be set, so that voltage on the capacitor would be virtually that of the input signal. When the "track" command came, the capacitor would hold the voltage from the instant before the voltage drop.



78-12-49

Figure 9 Pulse charge waveform with waveform from track-and-hold circuit.

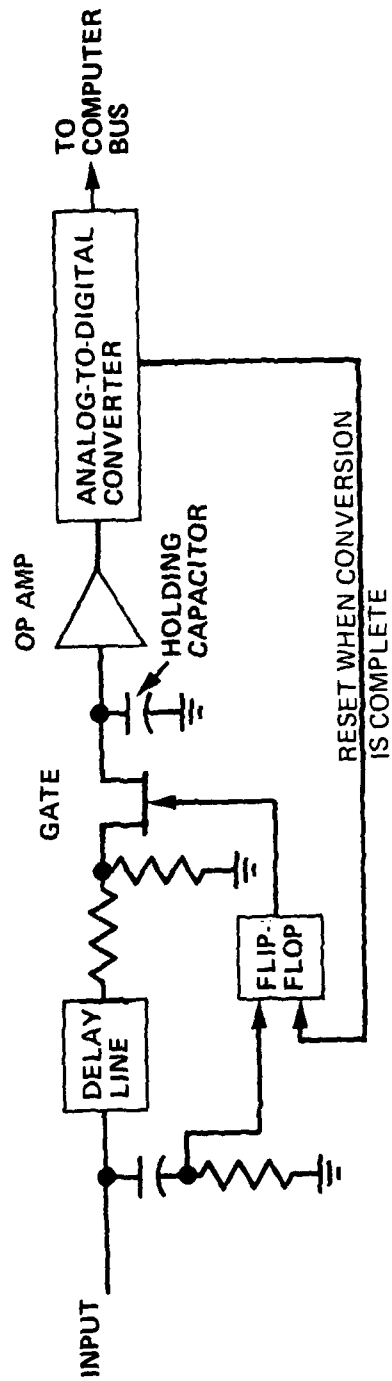


Figure 10 Block diagram track and-hold circuit for measuring pulse charge.

Switch Output Voltage Monitor.  $V_{In}$ , the voltage from the pulse forming line, is measured with a capacitive divider. Normally it does not vary in shape, only in amplitude, depending on the line switching voltage. This waveform can be adequately characterized by taking the integral of the trace electronically, unless switching anomalies slow the risetime of the pulse. The output voltage after the prepulse switch  $V_{IIn}$  is also measured with a capacitive divider. Variations in the amplitude of this wave are most likely to be caused by losses in the transmission line. The waveform can be elongated or shortened by variation in the prepulse switch hold-off time. Taking the integral of this voltage alone does not distinguish between these modes, but by measuring the time difference between the main switch closure and the prepulse switch closure, the two conditions could be distinguished by a simple algorithm. This time could be measured either at this point or at the diode; since there is a fixed distance and no switches between, the time difference should be no more than the spacing times the speed of light in water. If we measured the time of pulse arrival at both locations and set one for a long interval, we would have a means of determining if a malfunction occurred outside of our high-resolution time window. These measurements also provide a redundant time measurement in case of malfunction of the diode diagnostics.

Diode Diagnostics. These are monitors for diode (tube) voltage,  $V_{Tn}$ , diode current measured in the water,  $I_{Tn}$ , and current in the cathode,  $I_{cn}$ . Typical waveforms are shown in Figures 11a, 11b, and 11c along with waveforms of possible fault conditions. Measuring the areas under these curves, i.e., the integrals with integrating analog-to-digital converters, gives an adequate signature from each detector in the malfunction mode described. Conditions which these monitors are unable to distinguish are late-time diode shorts and otherwise normal shots into lower-impedance diodes. This is an important distinction, since the MBS spectrum



HORIZONTAL SCALE: 10 ns/DIV  
VERTICAL SCALE: ARBITRARY

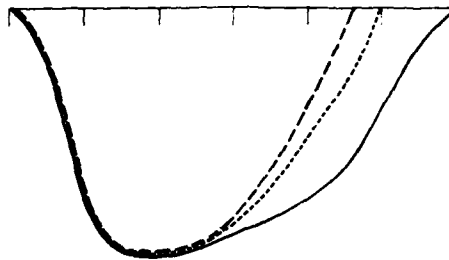


Figure 11a Diode voltage,  $V_I$ .

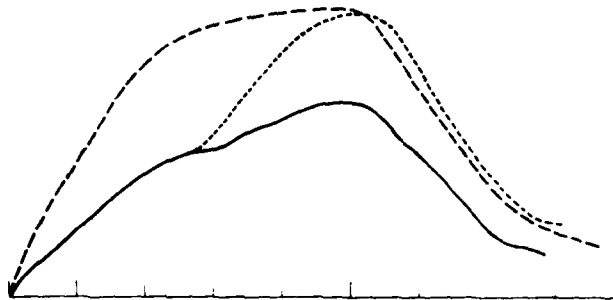


Figure 11b Diode current waveform,  $I_D$ .

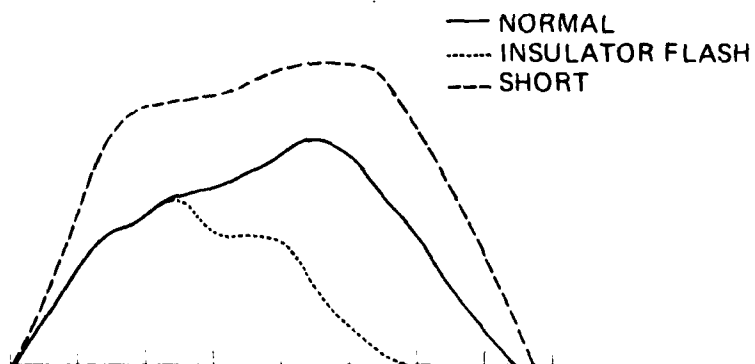


Figure 11c Cathode current,  $I_C$ .

78-12-51

can be considerably different in the two cases. It is possible that other circuits could be built that would distinguish between these conditions. An analog multiplier feeding into an integrating analog-to-digital converter would distinguish these modes. This would directly measure diode energy by taking the  $VIdt = \text{energy}$ .

Radiation Diagnostics. It would be very useful to have an on-line computerized set of radiation diagnostics for the convenience of facility users and ease of handling data in the development. This is a trivial computerized measurement to make since commercial modules are available. Since the signal is unipolar and does not oscillate like machine output signals, gating is no problem. The gate can be left open for a long period when one might expect a signal.

### 2.3 DATA INTERFACES

One decision that has to be made very rapidly when specifying a computerized data acquisition system is the type of interface with the computer. The interface is composed of the wiring diagram and card size for locating modules, supplying power, transmitting and receiving data, and indicating status. Most computer manufacturers offer their own interfaces. Computer manufacturers will generally try to confine the customer to their products as much as possible.

Two widely accepted interface standards exist. The one we propose to use is CAMAC (Computer Automated Measurement and Control), which was adopted in 1971 by the Committee of European Laboratories and the AEC. It is now standardized by the IEC (The International Electrotechnical Commission) and the IEEE in ANSI/IEEE standards 583-1975, 595-1976, 596-1976 and 683-1976.

The other is the HP-IB interface (IEEE 488). This interface is primarily used for small groups of laboratory instruments interfaced to a computer. It is limited to 15 devices, but many loops can be connected to a single computer. The HP-IB transmits 8 bits of data in a byte serial mode, but transmission distances are limited to 20 m.

CAMAC has the advantage over HP-IB that it is actually designed for large systems, such as the 3 to 5 thousand data channels that may be measured and controlled on the SXTF facility. It is also computer- and vendor-independent. Any vendor selling CAMAC instrumentation must meet CAMAC specifications for data transmission, power supplies, and module size and interconnection. Engineering and documentation for the interface were developed and paid for years ago. Now they are available for a nominal charge from the IEEE (\$20).

CAMAC systems are built around a "crate" which is a powered container holding the dataway, which is the wiring system to interconnect the modules. It has 25 slots for modules. The two right-hand slots accommodate a controller which interfaces the CAMAC system to a computer. At present there are probably controllers to interface six to eight types of computers. The remaining 23 slots will accept modules that are connected to the device being measured or controlled. (See Figure 12.)

The module can be queried if it is in position and ready to accept data. Alternatively each module is connected to the interface and can request attention if it has data. Data are transmitted or received on two 24-wire parallel data buses. All CAMAC modules are required to transmit a 24-bit word at a minimum transmission rate of 1 MHz. The 24-bit word is the decimal number 16,777,216, so it is adequate for any real-time data that we are ever likely

78-12-39

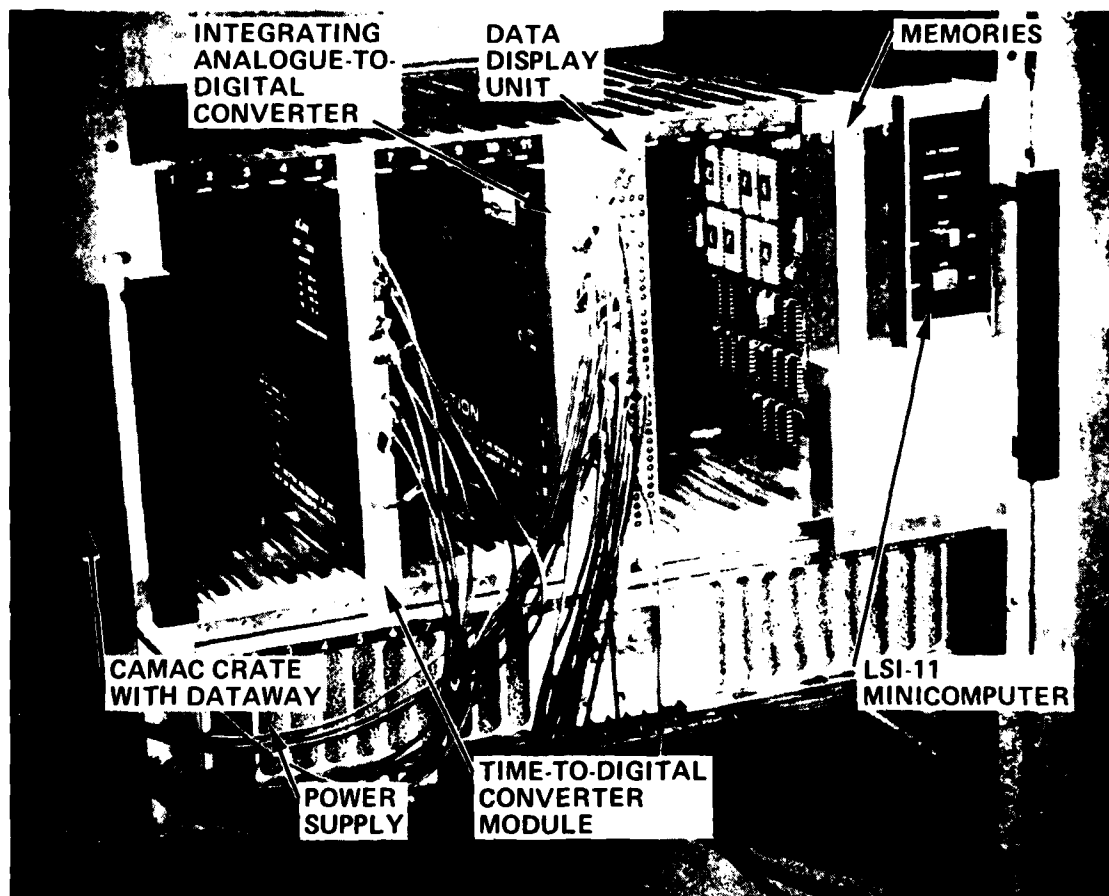


Figure 12 Prototype CAMAC data acquisition system.

to accumulate on our modules. In practice the computers that will probably be used on this type of system are 16-bit computers such as the PDP-1140 used in the DNA data acquisition system trailer at PI. Since the computer can directly address 16 channels per module in the crate, in principle it could directly address 368 discrete data channels per crate. Commercial hardware is available to drive up to 62 CAMAC crates in a serial system. Theoretically it would be possible with this 62-crate system to address 22,816 discrete data channels with the computer. We project that on the full 300-module MBS system, we will be interrogating approximately 3000 devices controlling another 500 to 1000 output units. The CAMAC serial data highway has adequate data capabilities for the type of system we are proposing. The cost without quantity discounts to implement one crate on a serial highway is \$3690. This unit will accommodate the 356 data channels and offers a fully interfaced and powered system for \$10.02 per channel.

The 4 modes of interfacing CAMAC crates to the computer are shown in Figure 13. A more complete description of the CAMAC interface is given in Reference 5. References 3 and 5 in the bibliography contain good articles on communications interfaces.

We recommend that the data acquisition system adopt the CAMAC format. All our projections and estimates are based on incorporation of a CAMAC system.

#### 2.4 GENERAL COMMENTS ON DATA ACQUISITION CIRCUITRY

The commercial hardware available is well conceived and versatile. Commercial time-to-digital converters are available from two vendors at \$150 per channel. Both would be very difficult to improve upon. They will resolve time differences of 100 picoseconds or less and are linear to  $\pm 0.1$  percent. We plan to use these units

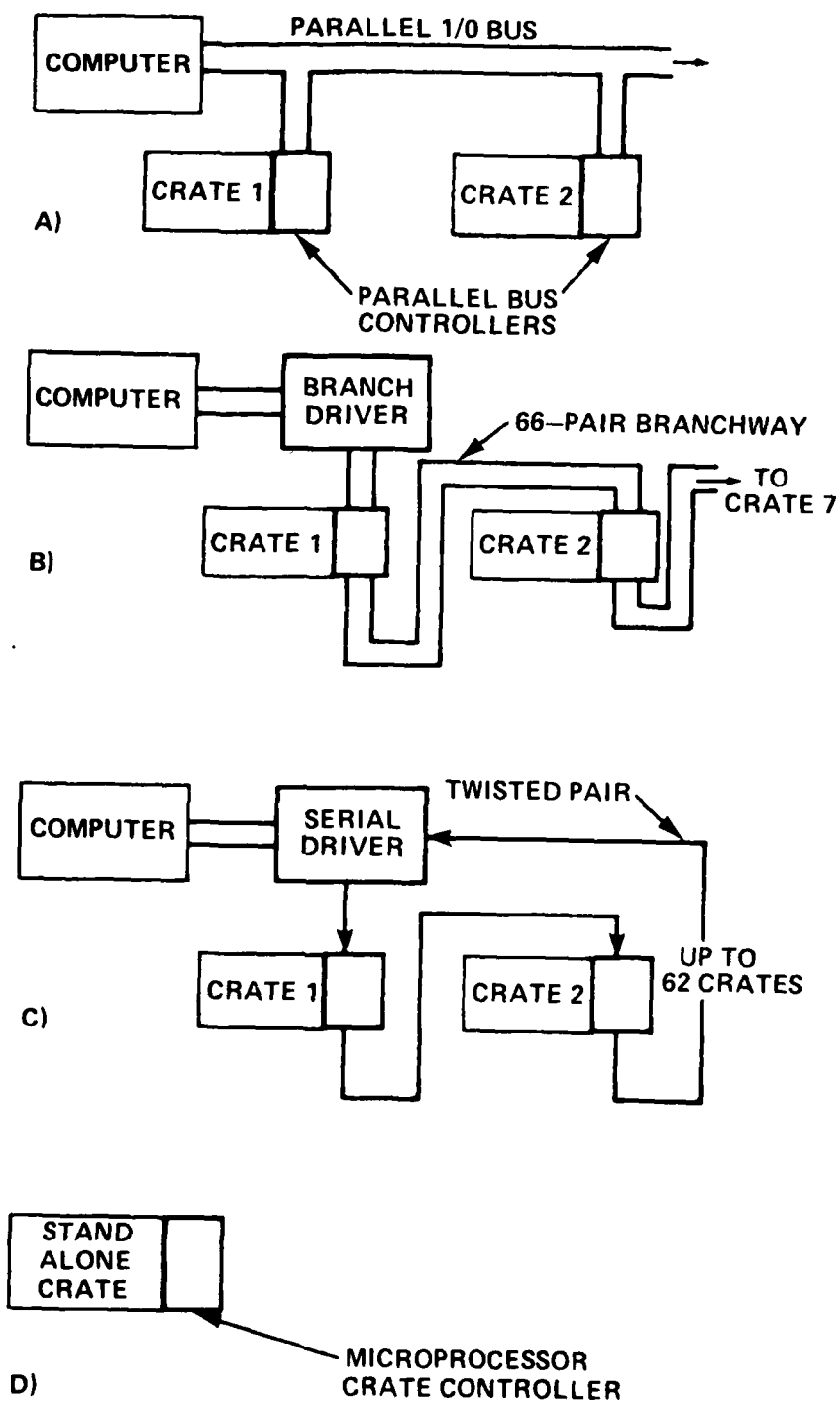


Figure 13 Methods of interfacing CAMAC to the computer.

to measure time intervals. The major improvements that could be applied to this hardware for MBS would be to increase the number of channels per CAMAC module, change to a much slower but cheaper analog-to-digital converter, and change to cheaper mass-terminated connectors. These modifications would probably lower the unit price to \$50-75 per channel.

Several versions of integrating analog-to-digital converters are available from different vendors. These units were designed for measuring the outputs of radiation detectors in nuclear accelerators. They have many features to provide versatility under a wide range of conditions, are very sensitive, and have high-repetition-rate capabilities. These analog-to-digital converters require inputs from peripherals, usually gating circuits. They cost from \$150 to \$170 per channel in small quantities without peripherals. For a system of less than 100 or 200 channels, it is reasonable to use these commercial units, since engineering costs are virtually zero.

Figure 14 is a schematic of diagnostics for an 8-module MBS system, using only commercial components. This diagnostic system has a commercial integrating analog-to-digital converter with separate gates on each channel. Gating would be done with a single discriminator gating  $V_{PC}$  and  $V_I$ . Another discriminator would be triggered by  $V_{II}$  and would gate  $V_{II}$ ,  $V_T$ ,  $I_I$  and  $I_C$ . Integrals of all trigger signals would be measured on a separate converter and gated by the master timing pulse.

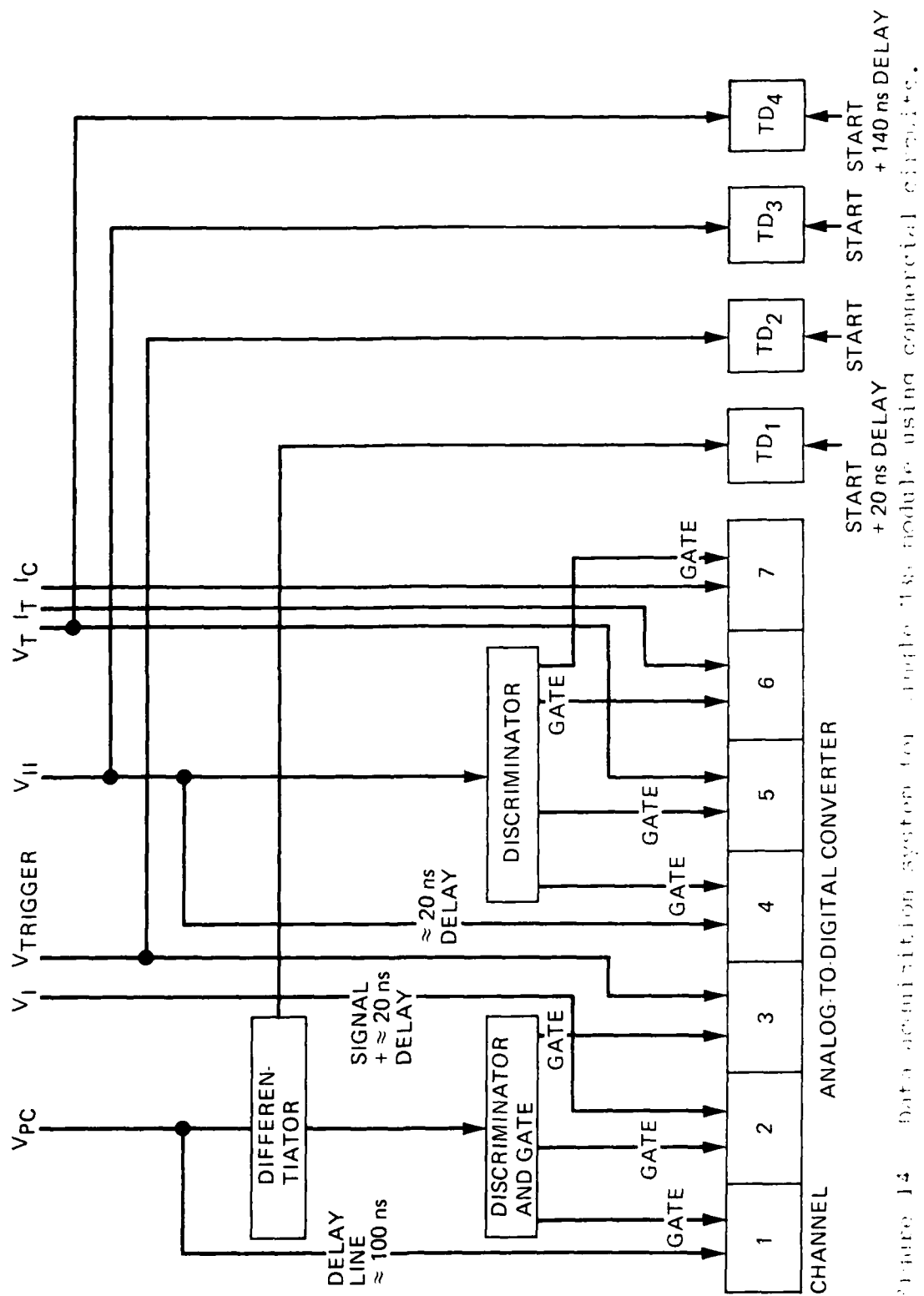


FIGURE 14 Data admission system for 400 ns module using commercial devices.



The cost for a single channel of this system is as follows:

Channel AD	\$170.00
Share of gate cost	55.00
Delay line (above normal)	20.00
Gate cable	10.50
Input passive electronics	<u>50.00</u>
	\$305.50 per channel plus crate and controller

For the 300-module MBS system, however, the most logical approach would be to design custom electronics. By designing the acquisition module functions required, such as the gating circuitry, a large amount of complex, space-consuming external hardware could be avoided. All the functions that data acquisition modules require could be incorporated, and many of the superfluous features of commercial units, which are added for the sake of versatility, could be eliminated.

Engineering costs to design custom circuits could not be amortized on only 8 modules; however, custom design would represent a considerable savings both in complexity and cost for a 300-module system. The circuitry would find application for any pulser, so the benefits would continue to accrue.

By incorporating the peripherals, such as gates and delays, into the CAMAC modules, costs on 2000 units could probably be reduced from \$305 per channel to about \$100.

## SECTION 3

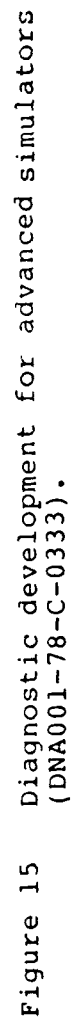
### EXPERIMENTAL PROGRAM

#### 3.1 PROGRAM PLAN AND OBJECTIVES

Our goal for the experimental program was to assemble an operating diagnostic system on the prototype MBS pulseline being assembled at PI in FY78. Our intentions were to:

1. Prove that the electronics and computer would function in the Pulserad environment
2. Prove that one could indeed diagnose a machine with the system
3. Develop experience to refine the diagnostic approach for the future MBS system.

When the contract was awarded, we prepared a program network that included having the prototype system fully operational and taking data within two months. Our original program plan is shown in Figure 15. We actually had the system on-line and operational four days ahead of schedule, and all three goals of the program were met. It should be emphasized that we had no intention of providing a highly refined system, but only proving feasibility. Every decision emphasized speed in achieving an operational system and maximizing the probability that the system would work.



### 3.2 COMPONENTS

CAMAC components were used to build up our prototype. These were chosen largely because: (1) a CAMAC-based diagnostic system could be built at minimum engineering cost; (2) CAMAC components were available from a local vendor, a factor that permitted quick turn-around in the event repairs were necessary; (3) CAMAC systems are available for the PDP-11 series computers that are used on other DNA facilities; and (4) CAMAC is also a modular standard in keeping with the philosophy of the MBS system.

A "stand-alone" system was purchased from a local vendor. This consisted of the following:

1. CAMAC crate
2. LSI-11 microcomputer repackaged by the vendor as a controller
3. Memories
4. Minimum software package burned into electrically programmable, read-only memory
5. A Dataway display to aid in determining system status.

Figure 12 shows the system fully assembled with an 8-channel time-to-digital converter and a 12-channel integrating analog-to-digital converter in place.

The converters chosen were commercial time-to-digital converters and integrating analog-to-digital converters, intended for use for particle counting in nuclear physics experiments. They were also purchased from a local supplier to minimize turnaround in case of malfunction.

The time-to-digital converter is an 11-bit (2048) converter, which has 0.048 percent resolution, and  $\pm 2$  count (0.096 percent) nonlinearity. It can be set for 100, 200, and 500 ns full-scale. The majority of our data were taken in the 200 ns scale, since we used the one converter to view the entire train of pulses propagating up the module. This technique gave a resolution of 100 ps.

The analog-to-digital converter is a 10-bit (1024) converter having a nonlinearity of  $\pm 0.25$  percent of reading ( $\pm 0.2$  percent of full-scale).

Tests of these accuracies on actual module pulses will be shown and tend to confirm these values.

### 3.3 DIAGNOSTIC MASTER TRIGGER

The time-to-digital converter required a common start timing pulse and the analog-to-digital converter a gating pulse to admit the signal to the integrator. Although commercial units are available that generate a low-voltage ( $-0.8$  V) gate, we chose to build a gate generator similar to the unit used to mark the oscilloscope traces. These units are virtually immune from damage by over-volting and do not emit repetitive outputs that cause spurious gating. They have jitter times on the order of a few picoseconds and an output of 80 volts, which can be used as the simultaneous start pulse for 800 time-to-digital converter channels.

### 3.4 FARADAY ENCLOSURES (SCREEN ROOMS)

Two complete shielded Faraday enclosures were built to shield the electronics from electromagnetic interference. The main enclosure was made large enough to accommodate visiting diagnosticians. It was used simultaneously by our data acquisition system and by Lockheed and ARACOR in turn when personnel from these companies took data on the MBS module.

We will illustrate the operation of our system with data from seven consecutive shots. These seven shots were chosen for illustration, since within these shots two distinct diode impedance conditions are shown, and three shots show diode insulator flashes. Also photos overlaying oscilloscope traces were taken, which illustrate very graphically the insulator flashes.

### 3.5 3-D RESULTS

Figure 16 shows a set of data taken with the computerized data acquisition system on a single module of the MBS system. It shows seven consecutive shots exhibiting four normal beam conditions and three pulses with insulator flashes. A schematic of the MBS module is shown with arrows pointing to diagnostic locations.

The Table in Figure 16 shows the output of the electronic sensors--the time in nanoseconds after the trigger and the integral of the pulse for every trace except the pulse charge. The integrals are in arbitrary units, since we did not fold in calibration factors on the sensors. Shots 706 and 707 are normal shots with a time spread of 1.5 to 2.0 ns between the pulses. The diode was opened at this point and readjusted. Shots 708 through 709 show an insulator flash in the vicinity of current monitor B. On shots 711 and 712, normal shots are obtained at a slightly higher diode impedance.

Below the tabulated data are overlays of oscilloscope traces from pulses 709 through 712. We can see that there is little difference between the tabulated integrals for  $V_{\text{pulse}}$  charge,  $V_1$ , and  $V_2$ . At first glance, the oscilloscope traces appear to be from one pulse, and the deviation on the integrals about 1/2 percent. The oscilloscope photo for  $V_T$  shows three distinct traces

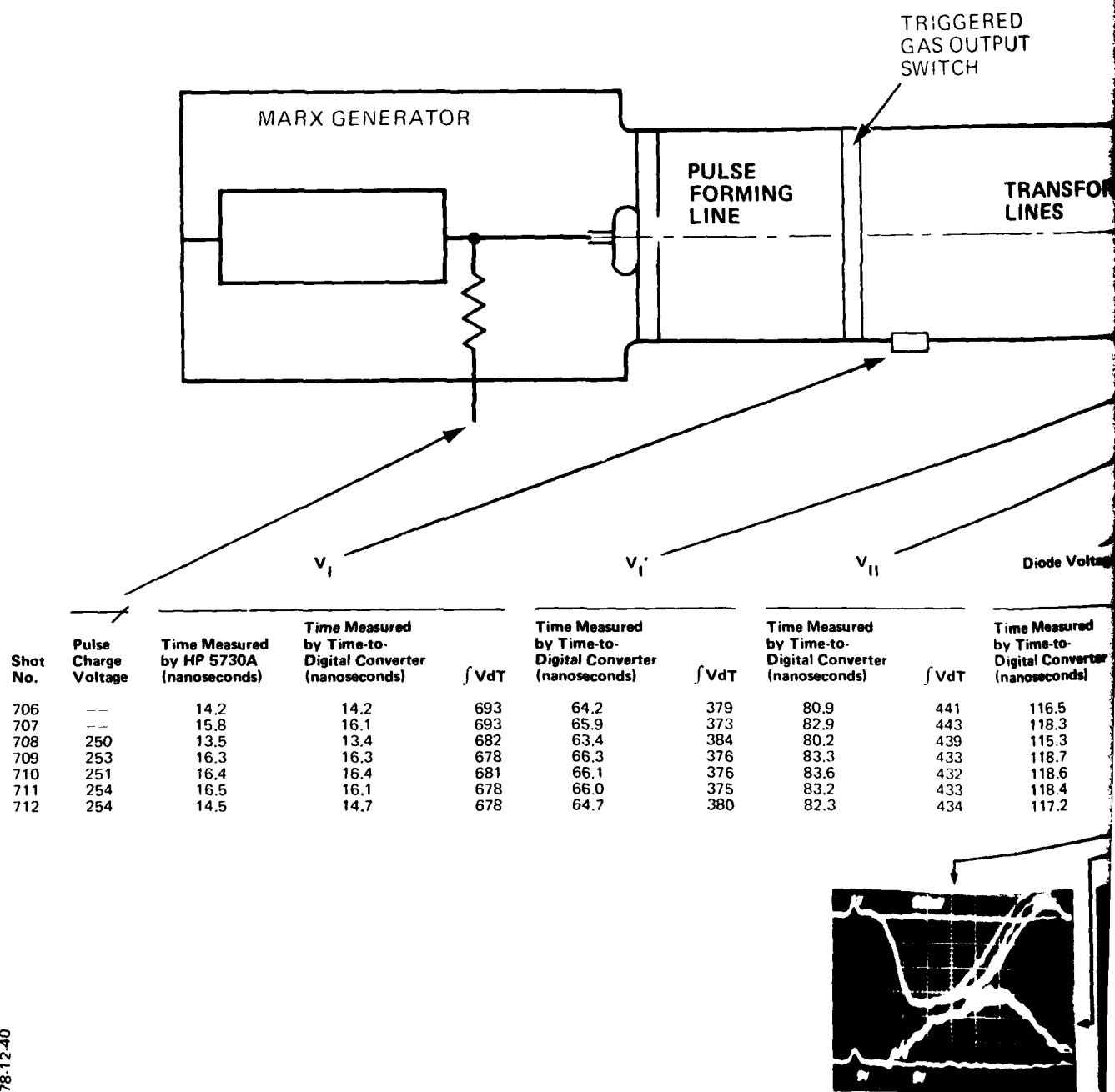
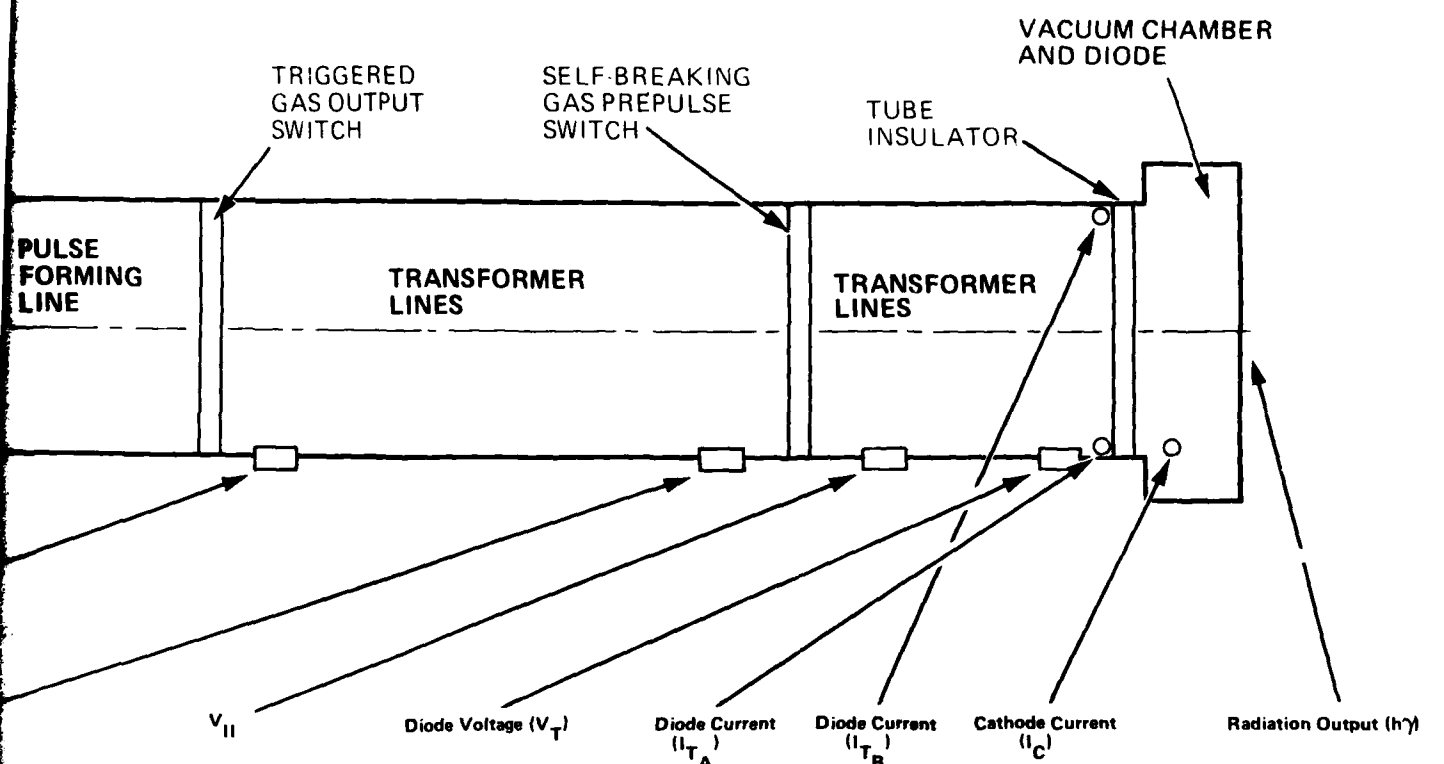
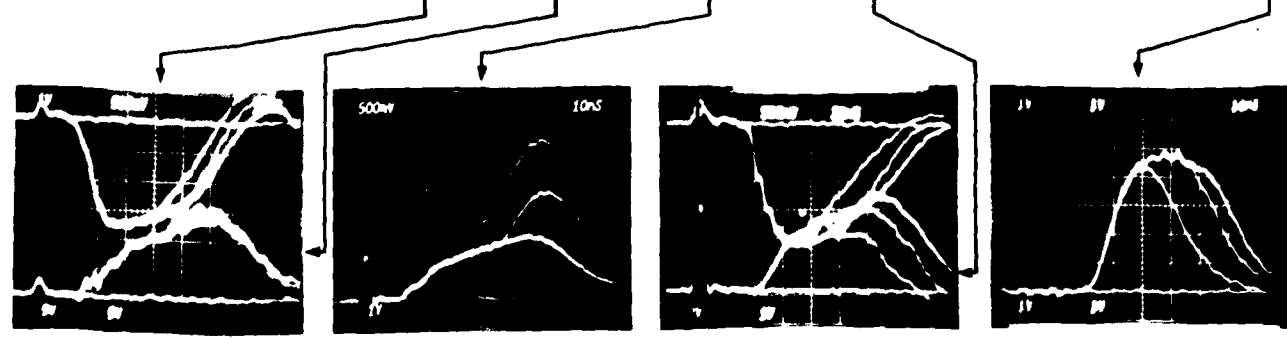


Figure 16 Summary of data from MBS pulses 706 to 712.



Time Measured by Time-to-Digital Converter (nanoseconds)		Time Measured by Time-to-Digital Converter (nanoseconds)		Time Measured by Time-to-Digital Converter (nanoseconds)		Time Measured by Time-to-Digital Converter (nanoseconds)		Time Measured by Time-to-Digital Converter (nanoseconds)	
$\int VdT$		$\int VdT$		$\int VdT$		$\int VdT$		$\int VdT$	
379	80.9	441	116.5	759	356	402	519	140.9	592
373	82.9	443	118.3	764	356	401	534	142.3	606
384	80.2	439	115.3	732	350	639	412	139.3	602
376	83.3	433	118.7	746	341	577	402	143.0	611
376	83.6	432	118.6	617	344	843	266	143.0	401
375	83.2	433	118.4	780	336	382	506	142.4	687
380	82.3	434	117.2	779	339	384	503	141.1	694





having the same peak amplitude, but beginning to drop to the baseline at different times. The wider trace appears brighter and is probably an overlay of traces 711 and 712. The integrals of  $V_T$  on shots 709 and 710 are indeed lower than those on shots 711 and 712.  $I_{T_A}$ , the current on one-half the diode shows little change both on the oscilloscope waveforms and digital outputs; however,  $I_{T_B}$  shows a much enlarged digital output on shots 709 and 710. The  $I_{T_B}$  oscilloscope traces show one heavy normal trace which is an overlay of pulses 711 and 712 and two lighter traces diverging to higher amplitudes about 25 and 35 nanoseconds into the pulse.  $I_C$  the current monitor on the diode past the diode insulator shows a drop in the integral of the current on pulses 709 and 710 from pulses 711 and 712, indicating a loss prior to the anode-cathode gap. The  $I_C$  waveform shows a bright, high-amplitude trace representing normal shots 711 and 712 and two distinct shorter lower-amplitude pulses.

The radiation diagnostics show correspondingly low outputs on pulses 709 and 710. There are no oscilloscope traces shown for shots 706 and 707, but they were normal shots with slightly lower voltage amplitudes as are the digital outputs. This condition implies a lower mean voltage, which probably caused the radiation outputs to be 13 percent lower than on shots 711 and 712.

Timing and synchronization of modules is very important for a pulser such as MBS. We use a "time-to-digital" converter to measure the time between the trigger pulse and the output pulse flowing in the line or radiation appearing at the target. The first two columns of Table 2 show a comparison of results for the time interval between the trigger and output voltage pulse in the line. The deviation between the measurements on the two detectors is a few tenths of nanoseconds. The timing data on voltage and radiation outputs follow.

TABLE 2  
NORMALIZED DATA FROM SHOTS 706 TO 712

	Delay, Trigger to $V_I$ (nanoseconds)		Radiation Output (nanoseconds)
	HP 5730A	Time-to-Digital Converter	
Mean Time Delay	15.33	15.31	141.7
Standard Deviation	1.20	1.21	1.35
Variance	1.26	1.26	1.57

It is quite obvious that the correlation between the Hewlett Packard 5730A counter and the time-to-digital converter (TDC) is good and also the jitter in radiation output is comparable to that of voltage out. A further check on our timing method is to measure the difference in time between monitors fixed in the line with no intervening switches. These pairs of monitors are  $V_2-V_1$  and  $V_T-V_3$ . Additionally we claim that the radiation output should occur a fixed time after the onset of voltage in the diode. These checks are stringent tests, since signals actually come from detectors on the pulser and are passed through the entire signal handling system.

Table 3 shows the data from shots 706 to 712.

TABLE 3  
DIFFERENCES IN TIME BETWEEN FIXED POINTS ON MBS  
(Times in Nanoseconds)

<u>Shot</u>	<u><math>V_I' - V_I</math></u>	<u><math>V_T - V_{II}</math></u>	<u><math>h\nu - V_T</math></u>
706	50.0	35.6	24.4
707	49.8	35.4	24.0
708	50.0	35.1	24.0
709	50.0	35.4	24.3
710	49.7	35.0	24.4
711	49.9	35.2	24.0
712	50.0	34.9	23.9
<hr/>			
Mean	49.91	35.23	24.12
Standard Deviation	0.122	0.25	0.21
Variance	0.0127	0.053	0.04

Since the least significant bit is 0.1 ns, these standard deviations are little more than quantized error.

## SECTION 4

### COST PROJECTIONS FOR THE SXTF

This program has demonstrated that module performance can be well documented using sensors at critical points and reading out key parameters with electronic circuitry. We feel that each of these circuits can be implemented in fully interfaced hardware for about \$100 to \$150 per channel. This program recommends the most cost-effective way to diagnose module performance that has been proven to function.

We will recommend a diagnostic system for the 300-module MBS proposed by Physics International. This diagnostic system could be used with other vendors' modules by using an analysis similar to that shown for PI's module.

First, we recommend a hardwired system to carry the fast analogue signals. A solid cable can be connected for about \$0.50 per foot and \$6.00 per connector. A 75-foot run with 4 connections would amount to about \$62.00 per cable. One must use reasonable care in cable and connector selection, cable routing, and use of a shielded enclosure for the readout system. No problems with our test system were encountered, even though the system was not optimized, as would be done in a newly designed facility.

Other potentially feasible types of systems are fiber optic systems and digital optical transmission systems. However, a fiber optic system is not recommended, since no large-scale analogue fiber optic systems have been developed commercially.

Digital optical transmission systems, which are much less complex than analogue systems, are commercially available for \$600 to \$800 per channel, exclusive of cable. Prices are continually decreasing, but it is unlikely that an analog optical transmission system at a reasonable price will be available in time to impact SXTF.

Secondly, we recommend the CAMAC System for the module diagnostic system. CAMAC is a well conceived system that has been in operation for a number of years--long enough to have been debugged. Since it is a nonproprietary, international standard system, procurement of components and parts can be made competitively; there would be no necessity to purchase from a particular computer vendor. Additionally, there are no engineering costs to set up the interfaces and protocols.

This system would have a block diagram similar to Figure 4 where the following parameters are monitored.

<u>Detector</u>	<u>Electronics</u>
$V_{PC}$	V at Breakback
$V_{Trigger}$	{ $\int Vdt$ Timing
$V_I$	{ $\int Vdt$ Timing
$V_{II}$	{ $\int Vdt$ Timing
$V_T$	{ $\int Vdt$ Timing
$I_T$	$\int Vdt$
$I_C$	$\int Vdt$

Summaries of costing for the modules and the Marx are shown in Tables 4 and 5.

TABLE 4

## MODULE DIAGNOSTICS FOR 300-MODULE MBS

<u>Item</u>	<u>Number Required per Module</u>	<u>Total Number Required</u>	<u>Estimated Cost per Item</u>	<u>Total Cost</u>
Sensors	Voltage Monitor Capacitive	4	1200	\$120,000
	Trigger Monitor	1	300	22,500
	Current Sensor Water	1	300	30,000
	Rogowski Coil Diode	1	300	60,000
Electronics	Cables	7	2100	129,150
	Timers	4	1200	120,000
	Breakback Track and Holds	1	300	30,000
	Integrator	6	1800	180,000
	Total			\$691,650

TABLE 5

MARX DIAGNOSTICS (38 MARXES)  
FOR 300-MODULE MBS

Item	Number Required per Marx	Total Number Required	Estimated Cost per Item	Total Cost
[Voltage Monitor	1	38	\$400	\$15,200
Trigger Voltage Monitor	1	38	75	2,850
[ $\int vdt$	1	38	100	3,800
Time-to-Digital Converter	1	38	100	3,800
Sample and Hold	1	38	125	4,750
Coaxial Cable	2	76	62	4,712
[Analogue-to-Digital Converters to Measure Charging Voltage and Current	4	152	22	3,325
Miscellaneous Cabling Shunts	4	152	20	3,040
Total				\$41,477

Sensors

Fast  
ElectronicsSlow  
Electronics

The system encompasses 3420 channels of fast instrumentation. If we assume that the mean number of channels per CAMAC module is 16, there are 214 modules. A reasonable guess would be that 20 modules would be installed per crate, so 11 crates and controllers would be required. These crate and interface hardware requirements are summarized in Table 6.

TABLE 6  
CAMAC CRATES AND INTERFACE HARDWARE

<u>Item</u>	<u>Number Required</u>	<u>Cost per Item</u>	<u>Total Cost</u>
Crate	11	\$1,995	\$21,949
Serial Driver	1	2,250	2,250
Controller	11	1,655	18,205
Cabling Termination	11	40	440
Terminator	1	275	<u>275</u>
			\$43,119

This configuration represents a minimum package interfaced to a serial port of a mini-computer such as a PDP-1140. The total cost does not include the cost of facilities software or engineering, since it is virtually impossible to price these items until they are defined. (See Table 7.)

TABLE 7  
PROJECTED TOTAL COMPONENT COSTS FOR MBS PULSER INSTRUMENTATION

Module Diagnostics, Cabling, and Instrumentation	\$691,650
Marx Electrical Diagnostics	41,477
CAMAC Crates and Interface Hardware	<u>43,119</u>
Estimated Total Component Cost	\$776,246

This cost estimate is exclusive of labor required for instrumentation system assembly and check-out.



The price estimates on the electronics are largely based on quantity discount prices for commercially available integrating digitizers and time-to-digital converters. The company which produces these digitizers and converters also produces similar modules for nuclear physics instrumentation with the high-density packaging and lower repetition rate that we require. These modules sell for about \$50 per channel in large quantities. They are not suitable for the MBS application without large amounts of peripheral hardware. However, their availability does suggest that the quantities of the type of units we require could be built for \$75 to \$100 per channel. Since in general the price of electronics is steadily decreasing, one could expect future reductions in cost rather than increases.

## BIBLIOGRAPHY

A series of general discussions of CAMAC are found in the following documents.

1. I.E.E.E. Transactions on Nuclear Science, CAMAC Tutorial Issue, April 1971, Volume NS-18, No. 2.
2. I.E.E.E. Transactions on Nuclear Science, CAMAC Tutorial Issue, April 1973, Volume NS-20, No. 2
3. J. Washburn, "Communications Interface Primer," Instruments and Control Systems, March 1978.
4. B. Zacharov, A Pedestrian's Guide to CAMAC, Science Research Council, Daresbury Nuclear Physics Laboratory, Daresbury, North Warrington, Lancashire, England.
5. H. J. Stuckenberg, CAMAC for Newcomers, DESY, Hamburg, West Germany, March 1975, Issue No. 13 of The CAMAC Bulletin, Supplement A.
6. R. Merritt, Universal Process Interfaces, CAMAC Vs HP-1B, Instrumentation Technology, August 1976.
7. The Standards for CAMAC are defined by the following I.E.E.E. Standards\*:
  - I.E.E.E. Standard 583-1975
  - I.E.E.E. Standard 595-1976
  - I.E.E.E. Standard 596-1976
  - I.E.E.E. Standard 683-1976

The following publications deal with voltage and current diagnostics.

8. D. Pellinen and S. Heurlin, "A Nanosecond Risetime Megavolt Voltage Divider," Review of Scientific Instruments, 42, No. 6, 824-827 (1971).

\*Available from I.E.E.E. Standards Office, 345 E. 47th Street, New York, N.Y. 10017.

9. D. Pellinen, "A Subnanosecond Risetime Fluxmeter," Review of Scientific Instruments, 42, No. 5, 667-670 (1971).
10. D. Pellinen and P. Spence, "A Nanosecond Risetime Megamp Current Monitor," Review of Scientific Instruments, 42, 11, 1699-1701 (1971).
11. D. Pellinen and I. Smith, "A Reliable Multimegavolt Voltage Divider," Review of Scientific Instruments, 43, No. 2, 299-301 (1972).
12. D. Pellinen, "A Segmented Faraday Cup to Measure  $\text{FA}/\text{cm}^2$  Electron Beam Distributions," Review of Scientific Instruments, 43, 11, 1654-1658 (1972). (Note: this contains the derivation for a differentiating fluxmeter or Rogowski coil.)
13. D. Pellinen and V. Staggs, "A Technique to Measure High Power Electron Beams," Review of Scientific Instruments, 44, No. 1 (1973). (Note: this has the equations for a self-integrating Rogowski coil such as we plan to use for the diode.)

## DISTRIBUTION LIST

### DEPARTMENT OF DEFENSE

Assistant to the Secretary of Defense  
Atomic Energy

ATTN: Executive Assistant

Defense Nuclear Agency

ATTN: DDST

4 cy ATTN: TITL

3 cy ATTN: RAEV

Field Command

Defense Nuclear Agency

ATTN: FCPR

Field Command

Defense Nuclear Agency

Livermore Division

ATTN: FCPRL

Defense Technical Information Center

12 cy ATTN: DD

Undersecretary of Def. for Rsch. & Engrg.

ATTN: Strategic & Space Systems (OS)

### DEPARTMENT OF THE ARMY

Harry Diamond Laboratories

Department of the Army

ATTN: DELHD-N-P

### DEPARTMENT OF THE NAVY

Naval Surface Weapons Center

ATTN: Code F31

### DEPARTMENT OF THE AIR FORCE

Air Force Weapons Laboratory

Air Force Systems Command

ATTN: SUL

### DEPARTMENT OF DEFENSE CONTRACTORS

Advanced Research & Applications Corporation

3 cy ATTN: Document Control

General Electric Company-TEMPO

ATTN: DASIAC

IRT Corporation

ATTN: Document Control

JAYCOR

3 cy ATTN: Document Control

Maxwell Laboratories, Inc.

ATTN: Document Control

Mission Research Corporation

ATTN: Document Control

Physics International Company

ATTN: D. Pellinen

ATTN: S. Ashby

R & D Associates

ATTN: C. MacDonald